



A Review on VTOL Autonomous Landing Strategies on Naval Dynamic Surfaces

- Luis Gustavo Leandro de Paula** PhD student, Cranfield University, School of Aerospace, Transport and Manufacturing, MK43 0AL, Cranfield, UK. luis.leandrodepaula@cranfield.ac.uk
- Vijay Shankar Dwivedi** Research Fellow, Cranfield University, School of Aerospace, Transport and Manufacturing, MK43 0AL, Cranfield, UK. VijayShankar.Dwivedi@cranfield.ac.uk
- Hyo-Sang Shin** Professor, Cranfield University, School of Aerospace, Transport and Manufacturing, MK43 0AL, Cranfield, UK. Professor, Cho Chun Shik Graduate School of Mobility, KAIST, Daejeon 34141, Republic of Korea h.shin@cranfield.ac.uk
- Antonios Tsourdos** Professor, Cranfield University, School of Aerospace, Transport and Manufacturing, MK43 0AL, Cranfield, UK. a.tsourdos@cranfield.ac.uk

ABSTRACT

Over the past decade, autonomous Vertical Take-Off and Landing (VTOL) aircraft have been increasingly operated in a wide range of applications in both civil and military markets. Nevertheless, shipboard missions represent a notably demanding operational scenario when it comes to the landing procedure. Autonomous solutions must consider complex landing pad dynamics, vessel air wake, wind disturbances, and challenging environmental conditions. This paper presents a review of autonomous landing strategies on naval dynamic targets, covering solutions based on Relative Navigation Systems, Computer Vision, LiDAR, Physical Interfaces, and Robotic Landing Gears. A total of 56 publications were reviewed based on control design, landing platform motion fidelity, hardware requirements on the deck, and test assumptions. Further assessment investigated the autonomous level and landing criteria while comparing the performance of flight-tested control methodologies. Finally, this paper provides an overview of shipboard autonomous landing research and outlines future challenges to expand operations in harsh sea conditions.

Keywords: Autonomous; Landing; UAV; Shipboard

Nomenclature

<i>AHC</i>	= Active Heave Compensation	<i>AR</i>	= Autoregressive Models
<i>CEP</i>	= Circular Error Probability	<i>CV</i>	= Computer Vision
<i>DA</i>	= Direct Approach	<i>DL</i>	= Datalink
<i>EKF</i>	= Extended Kalman Filter	<i>EW</i>	= Empty Weight
<i>FC</i>	= Flight Controller	<i>FH – MPC</i>	= Fixed Horizon MPC
<i>FF – IBVS</i>	= Feed Forward IBVS	<i>FoV</i>	= Field of View
<i>FT</i>	= Flight Test results	<i>Pr</i>	= Procedure type

<i>GT</i>	=	Ground Test results	<i>GNC</i>	=	Guidance, Navigation and Control
<i>HW</i>	=	Hardware	<i>IBVS</i>	=	Imaged Based Visual Servoing
<i>KF</i>	=	Kalman Filter	<i>LPI</i>	=	Landing Period Indicator
<i>MCA</i>	=	Minor Component Analysis	<i>MC</i>	=	Motion Capture System
<i>MLE</i>	=	Maximum Landing Error	<i>ML</i>	=	Machine Learning
<i>MPC</i>	=	Model Predictive Control	<i>MRAC</i>	=	Model Reference Adaptive Control
<i>MPC – NE</i>	=	MPC with Nonlinear Estimator	<i>NVD</i>	=	Night Vision Device
<i>NP</i>	=	Nonlinear Programming	<i>PBC</i>	=	Park Braking Control
<i>PH</i>	=	Prediction Horizon	<i>QP</i>	=	Quadratic Programming
<i>RAO</i>	=	Response Amplitude Operators	<i>RLG</i>	=	Robotic Landing Gear
<i>SH – MPC</i>	=	Shrinking Horizon MPC	<i>SHOL</i>	=	Ship Helicopter Operation Limitation
<i>SIM</i>	=	Simulations results	<i>FC</i>	=	Flight Controller
<i>SS</i>	=	Sea State	<i>S, Sw, H</i>	=	Surge, Sway, Heave
<i>TDP</i>	=	Touch-Down Point	<i>UWB</i>	=	Ultrawideband
<i>USV</i>	=	Unmanned Surface Vehicle	<i>V&V</i>	=	Verification and Validation
<i>VA</i>	=	Vertical Approach	<i>VoV</i>	=	Verification and Validation
<i>VH – MPC</i>	=	Variable Horizon MPC	<i>VMC</i>	=	Visual Mode Control
<i>VTOL</i>	=	Vertical Take off and Landing	<i>WMO</i>	=	World Meteorological Organization
<i>g</i>	=	gravity	<i>S(ω)</i>	=	Wave spectra function
<i>ω</i>	=	Wave frequency	<i>ω_m</i>	=	Wave modal frequency
<i>ω_e</i>	=	Wave encounter frequency	<i>U₀</i>	=	Vessel forward speed
<i>χ</i>	=	Wave encounter angle	<i>ω_e</i>	=	Wave encounter frequency
<i>P, Y, R</i>	=	Pitch, Yaw, Roll	<i>X, Y, Z</i>	=	Surge, Sway and Heave

1 Introduction

During the last decade, autonomous Vertical Take Off and Landing (VTOL) aircraft have increasingly been employed in a wide range of applications, both in civil and military markets [1]. Small-scale Unmanned Aerial Vehicles (UAVs) moved from fixed-wings to multi-rotors mainly due to onboard processing capabilities and innovations in computer vision [2]. However, full-scale UAVs based on conventional manned helicopters [3, 4] were still being designed, since more development effort can be spent on the autonomous flight control technology rather than airworthiness [5]. One challenging mission scenario for UAVs is offshore operation. Typical ship-based VTOL UAV missions include search and rescue [6], surveillance and reconnaissance, industry inspection, and others like wildlife and iceberg monitoring [7].

Traditionally, ship-board take-off (launch) and landing (recovery) operations are considered demanding tasks even for skilled helicopter pilots [8]. Compared to land-based procedures, these tasks are also challenging for autonomous systems due to the unique set of conditions. Shipboard operations require landing on a 6 DoF moving target under complex air wake, water sprays, fog, and low-level ambient light [9, 10]. Offshore landing platforms include not only large-scale vessels, but also autonomous water Unmanned Surface Vehicle (USV) and docking stations that can be used as a central operation node [11].

The challenge of operating UAVs from shipboard platforms is not new. The DASH program in 1960 introduced one of the first VTOL UAVs designed for shipboard operations [12]. The QH-50 coaxial rotorcraft, with over 700 units produced, was remotely piloted from deck stations and had a significant legacy to autonomous rotorcraft programs. However, operational policies led to the loss of over 400 drones, prompting the U.S. Navy to halt the program in 1971 [13]. Since then, more recent autonomous and remotely piloted rotorcraft, such as the MQ-8C helicopter, have been introduced into service [5].

Yet, robust interface designs and safe UAV landings under severe weather conditions and high sea states remain challenging [6, 14].

During the past decade, the increased availability of small-scale UAVs has led to many flight-tested solutions that aimed to improve the landing envelope under adverse conditions. These publications were often based on subscale vessel scenarios or cooperative water USVs. Furthermore, various strategies, such as robotic landing gears and GNC based on computer vision, have been enhanced from an airworthiness perspective [3, 15]. Additionally, research has explored collaborative control frameworks between USVs and UAVs, as evidenced by comprehensive literature reviews [11, 14]. However, achieving optimal landing conditions may not always be feasible due to the vessel's operational requirements, especially for heavy-class UAVs under high sea states [10]. In [16], the authors listed several research directions for UAV autonomous landing strategies on dynamic targets, including external assisting systems for relative navigation, guidance based on visual cues, multi-sensor data fusion, and learning-based control methods. Further details on vision-based approaches can be found in reviews covering autonomous landing techniques addressing static and moving targets on the ground [16, 17]. In these publications, key performance criteria for shipboard operations are mainly based on landing accuracy, time required to land, or success rate, particularly for techniques relying on vision-based technologies.

To our knowledge, there is no comprehensive literature survey that offers an overarching view of sensors, Guidance, Navigation, and Control (GNC), and the specific landing criteria for VTOL UAVs when landing on moving platforms exposed to ship motion. Furthermore, this paper proposes a classification that covers both the fidelity of target dynamics and the relevant landing criteria, while providing a performance comparison between the higher fidelity flight tests. These features are of key importance when considering landing pads that are under harsh sea state conditions. Therefore, this paper's main contribution is to offer insights into research trends and future challenges for rotorcraft GNC solutions focused on autonomous shipboard landings. A broader overview is given by covering the following strategies: Relative Navigation systems, Robotic Landing Gear, Computer Vision, LiDAR-based, and Physical Interfaces.

This paper is organized as follows: Section 2 discusses essential parameters and conditions related to UAV shipboard operation that are relevant to the literature review, Section 3 presents the literature classification strategy and the main results, Section 4 provides a comparison study with insights into future challenges and research gaps, and Section 5 presents the concluding remarks.

2 Overview of Shipboard Autonomous Landing

The determination of the flight envelope for helicopter shipboard operations is influenced by four primary factors, as outlined in [10]: the helicopter's flight characteristics and limitations, atmospheric conditions, the ship environment, and the pilot's interaction with the helicopter. As illustrated in Fig. 1, numerous considerations must be addressed during qualification tests to assess the compatibility between a particular helicopter and ship.

Besides the wind and ship structure complex interaction, flight deck dynamics can also be a limitation for shipboard landing and take off procedures. The operating envelope is typically defined based on wind parameters and ship motion such as [19]: pitch angle, roll angle, flight deck lateral acceleration, and flight deck vertical acceleration. Large attitudes could lead to unsafe conditions which include rollover, sliding, or exceeding design loads of the landing gear. Typical SHOL values for civil operation can be found in [20], while for military operation are presented in [21]. However, it must be noted that these parameters heavily rely on the ship and rotorcraft interface. Standard landing and take-off procedures for heavy class helicopters are presented in Fig. 2. A common feature is that the landing is always performed from a hover position above the deck. In emergency scenarios such as single-engine, the astern procedure

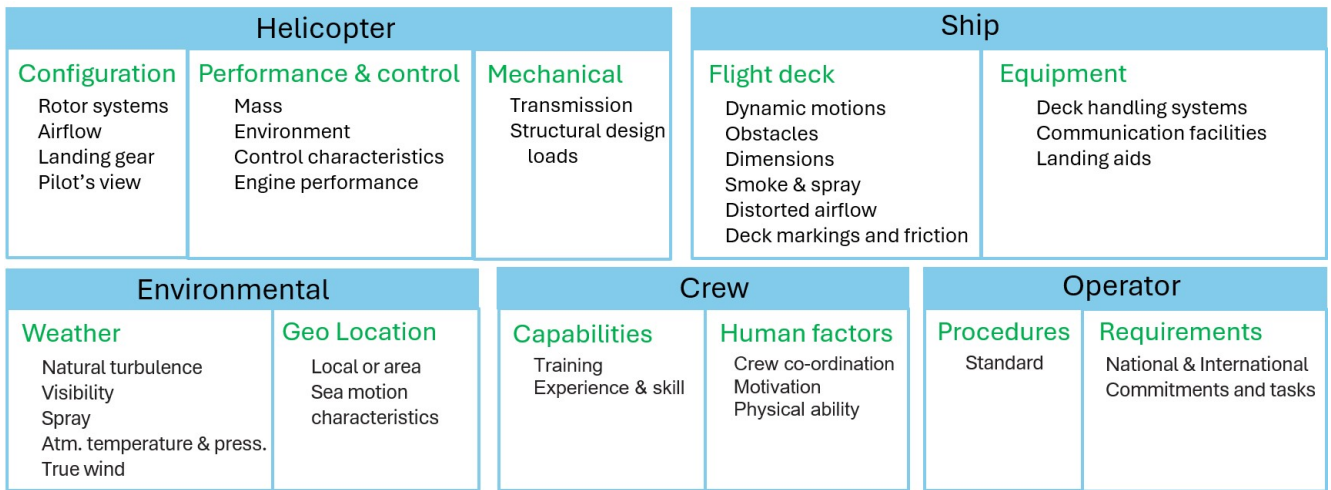


Fig. 1 Factors affecting ship-borne helicopter operations [18].

is performed with maximum vessel speed and lowest helicopter operational weight to improve hover performance.

Table 1 Example of SHOL limits for landing on ships other than carriers [21]

Configuration	Day		Night (Conventional)		Night (NVD)	
	Pitch	Roll	Pitch	Roll	Pitch	Roll
Skid / Narrow Wheel / High C.G. / Tail Wheel	$\pm 1^\circ$	$\pm 3^\circ$	$\pm 1^\circ$	$\pm 2^\circ$	$\pm 1^\circ$	$\pm 2^\circ$
Wheel without deck securing system	$\pm 2^\circ$	$\pm 4^\circ$	$\pm 1^\circ$	$\pm 3^\circ$	$\pm 1^\circ$	$\pm 3^\circ$
Wheel with deck securing system	$\pm 2^\circ$	$\pm 6^\circ$	$\pm 1^\circ$	$\pm 4^\circ$	$\pm 1^\circ$	$\pm 4^\circ$

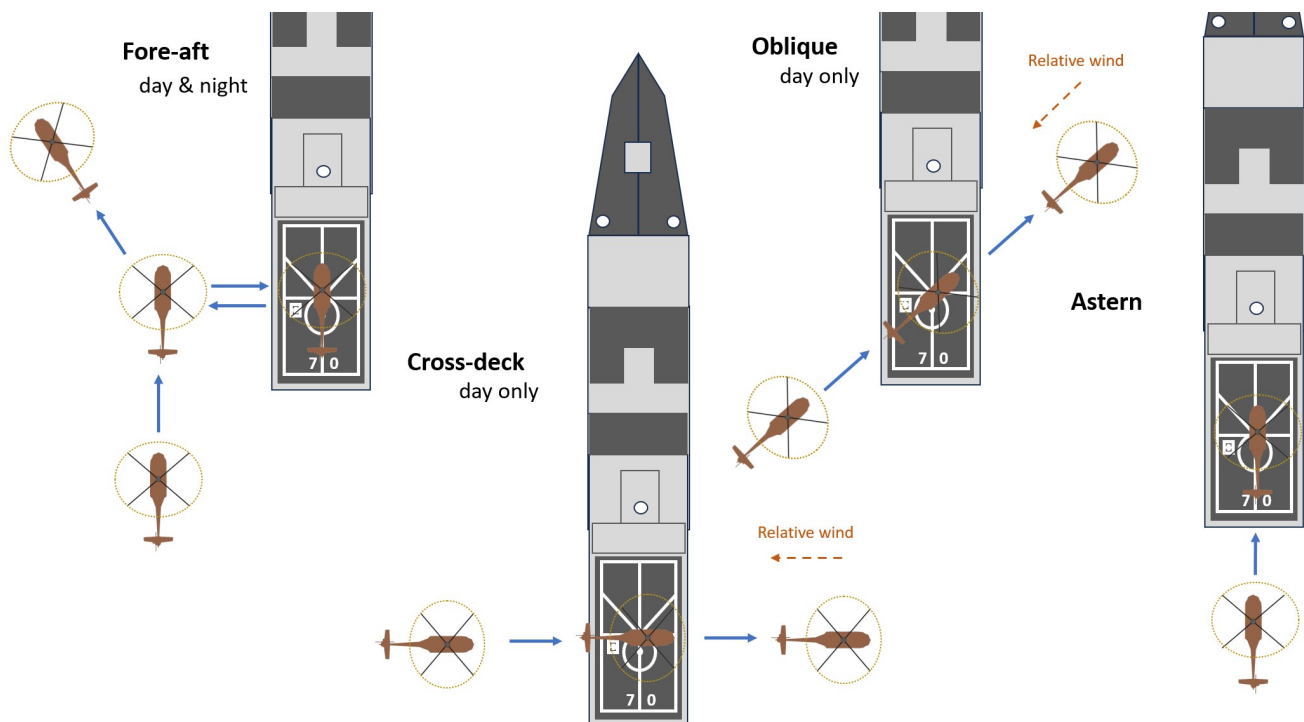


Fig. 2 Standard landing and take-off procedures [18].

In shipboard operations, the landing platform motion can be considered highly complex due to the intrinsic random nature of waves. Usually, wave models are based on spectral energy distributions such

as JONWASP, Bretschneider, or Pierson-Moskowitz. In turn, these distributions usually rely on sea state empirical parameters that capture characteristics such as significant wave height and model wave periods [22]. The World Meteorological Organization (WMO) provides a sea state code (SS) that is widely adopted, and it is based on wave height and visual characteristics as defined in the international code standards (Code 3700) [23]. Moreover, the correlation between SS and wave modal period and significant wave height can be found in [22, 24]. For instance, the ship response to wave dynamics can be characterized by Response Amplitude Operators (RAO) transfer functions, which rely on wind, ship heading, and ship velocity. Manufacturers usually issue tabulated data based on experimental and numerical identification [25].

Before presenting the literature search criteria and classification strategies, it is important to understand which landing pad DoF shall be considered to perform a proper analysis under harsh sea state conditions. Using the same approach as [26], the Bretschneider wave spectra $S(\omega)$ for fully developed long-crested seas can be described by Eq.1, where ω is the wave frequency, ω_m is the modal frequency and $H_{1/3}$ is the significant wave height. The simulated parameters are the mean values for North Atlantic Sea presented in [22], where the relation between $H_{1/3}$, ω_m , sustained wind speed, and the sea state code can be found.

$$S(\omega) = \frac{5}{16} \frac{\omega_m^4}{\omega^5} H_{1/3}^2 e^{-5\omega_m^4/4\omega^4} \quad (1)$$

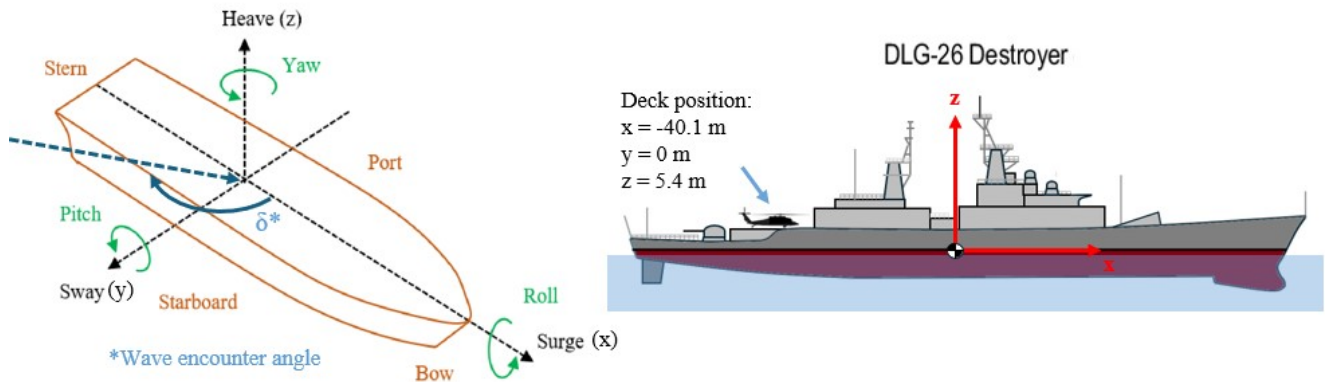
Moreover, the spectrum observed by a ship traveling with forward speed U_0 is affected by the Doppler shift. Considering a model of sea elevation as numerous independent regular contributions of random phases, as stated in [27] the spectra can be described as in Eq. 2, where χ is the wave encounter angle and ω_e is the wave encounter frequency.

$$S(\omega_e, \chi) = \frac{S(\omega, \chi)}{|1 - (2\omega U_0/g) \cos \chi|}, \quad \omega_e = \omega - \frac{\omega^2 U_0 \cos \chi}{g} \quad (2)$$

Considering a destroyer class vessel (USS DLG-26) based on RAO tables [28, 29] and Bretschneider wave spectra [22], simulations results are given in Fig. 3 for both SS 2 (calm sea) and SS 6 (harsh conditions) along with definitions of ship axes and the deck position.

From Fig. 3 the heave motion plays an important role mainly in the lower sea states (<3), while pitch and roll also become relevant for the higher sea states (>5) [30]. Control responses tailored for surge, sway, and yaw are generally not applied to larger ships, as these movements are seldom pronounced, even under harsh sea state conditions such as SS 5 [31]. One important feature, however, is that RAO works as a low-pass filter for large-scale vessels, and, as a result, short-term state predictions can be performed even without the platform dynamics [32]. While one of the criteria for paper selection is that the landing pad motion includes at least heave, pitch or roll oscillations, for high sea state condition oscillations of roll and heave DoF should not be neglected when considering high sea state evaluation.

As a selection criterion, only publications featuring at least one of the following: heave, pitch, or roll oscillations, were considered. Alongside the landing pad DoF, publications were initially chosen based on aircraft configuration, given the focus on VTOL UAVs. No restrictions were imposed regarding weight class or dimensions, aiming to offer an overview across both low- and real-scale test scenarios. Additionally, priority was placed on close-range Guidance, Navigation, and Control (GNC) solutions for the landing procedure, a critical phase of shipboard operations. Only publications demonstrating at least basic fidelity of the target dynamics were included to properly evaluate test limitations regarding harsh sea state conditions. The database comprised both flight-tested solutions, aimed at identifying operational gaps, and simulation-based research exploring proof of concepts for novel approaches. This included



DLG-26 Destroyer class, center deck position, Wave encounter = 150° , Speed = 10 kt

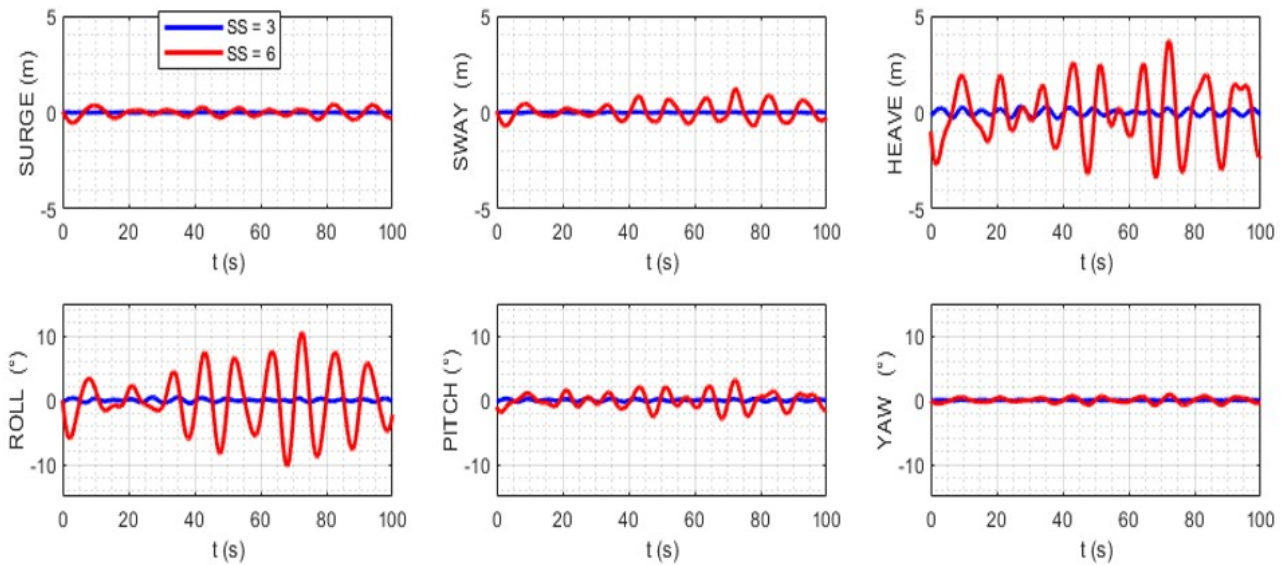


Fig. 3 Ship motion example in different sea state conditions.

both automatic and autonomous GNC strategies, as well as solutions offering alternative methods of controlled compensation for landing pad oscillations, such as active mechanical interfaces.

A high-level overview of the publication criteria is provided in Fig. 4. It should be noted that autonomous and automatic approaches that assumed the ship states were readily available were not included in the database. The main reason is to focus on integrated solutions that also address the sensing and estimation of ship states. Recent research has shown a focus on flight testing in challenging sea states, leading to the selection of publications from the past decade. The detailed PRISMA identification and screening process can be found in Fig. A1, which includes a list of searched keywords, publication databases, and specific exclusion reasons. As a result, 56 publications were screened, of which 35 were selected to represent the most recent findings from their respective research groups. These selected publications are summarized in Table A1.

3 Literature Review

One of the most critical requirements of autonomous shipboard operations is to rely on minimal or even no hardware installed on the deck [3]. The main goal is to enhance interoperability across different navy platforms. On the other hand, accurate pose estimation usually relies on the installation of support hardware on the deck. Since sensor selection for pose estimation is closely related to the ship hardware requirements, the suggested literature analysis was classified into the following groups

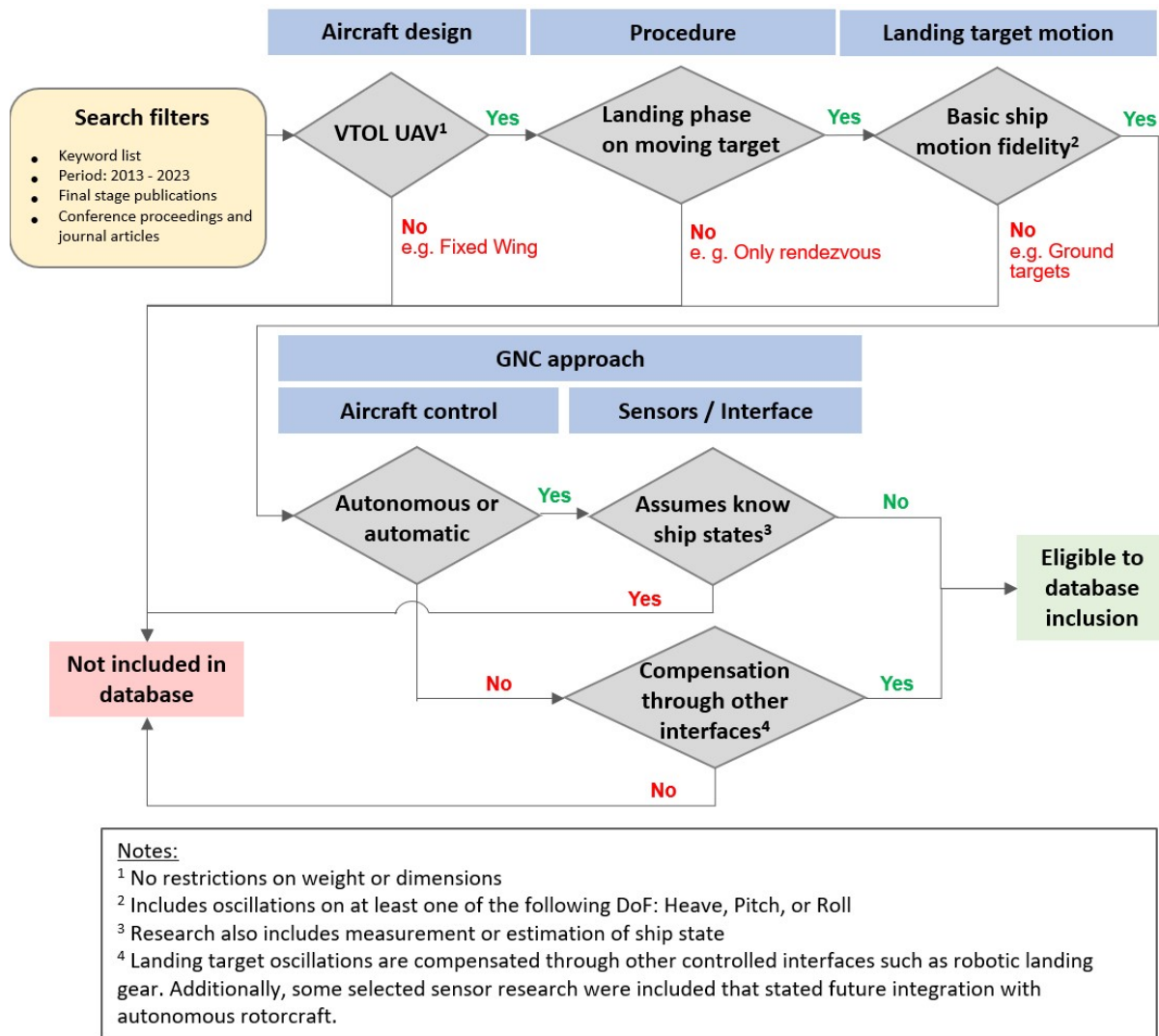


Fig. 4 High level screening criteria of publications.

of sensing modalities: LiDAR, Computer Vision (CV), and Relative Navigation (RelNav). Moreover, two different interface approaches were also identified: active-controlled Physical Interfaces and Robotic Landing Gear (RLG). This classification was also based on the fact that fewer publications addressed a combined interface framework within these groups. It should be noted that these frameworks are not alternates, but can be regarded as complementary. However, this classification provides useful insights into the different strategies presented in the literature. A distribution of the previous classified groups is presented in Fig. 5.

Research papers were further classified into categories outlined in Table 2. Three key aspects were taken into account: the autonomous level of the GNC solution, the definition of the landing criteria, and the landing pad DoF. The heave and roll oscillations were deemed as minimal representations of harsh sea state conditions and were therefore assigned a specific class in terms of landing pad DoF fidelity

A historical overview of the selected publications is given in Fig. 6. It can be seen that there is an increase in research groups exploring autonomous landing on naval dynamic surfaces. Additionally, there is a high number of publications that rely on GNC approach based on CV sensors, which may be related to the fact that this is the least expensive interface strategy for pose estimation. The classification based on the proposed categories in Table 2 is presented in Fig. 7. Research group publications were further organized and classified as per Table A1. Following subsections will present details of each interface strategy along with their background.

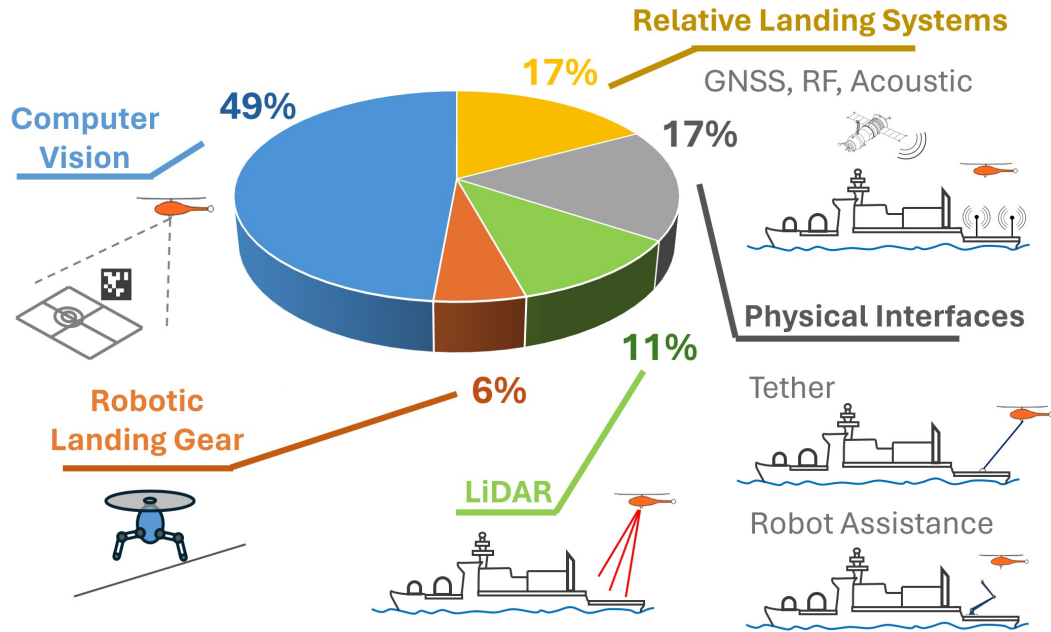


Fig. 5 Distribution of Autonomous Landing solutions by interface approach.

Table 2 Classification categories based on autonomous level, landing criteria and landing pad DoF

Category	Autonomous Level	Landing criteria	Landing pad DoF fidelity
I.1	Fully autonomous	Based on forecasted target states	Considers at least heave and roll oscillations
I.2			Other set of ship DoF oscillations
II.1	Fully autonomous	Based on current target states or other criterias (e.g. spatial threshold)	Considers at least heave and roll oscillations
II.2			Other set of ship DoF oscillations
III	Partially autonomous or automatic procedure	Triggered by external operator	Considers at least heave or roll oscillations
IV	Research focused on active compensation interface	Not applicable	Not applicable

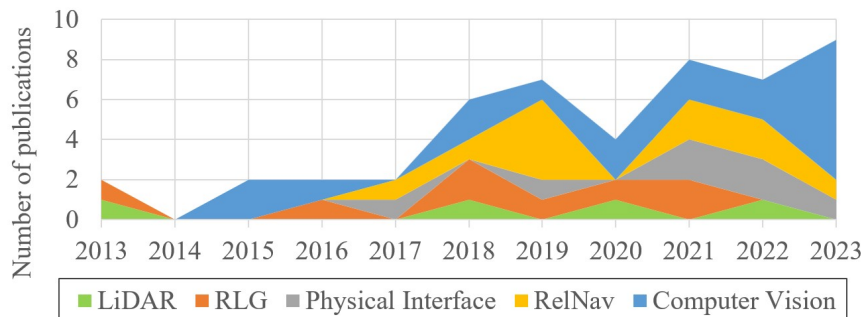


Fig. 6 Publications over the last 10 years by interface strategy.

3.1 Robotic Landing Gear (RLG)

One technology that has been further investigated in the past decade is the Robotic Landing Gear (RLG) system. In [33], the authors demonstrated an increase in the slope landing envelope with a four-

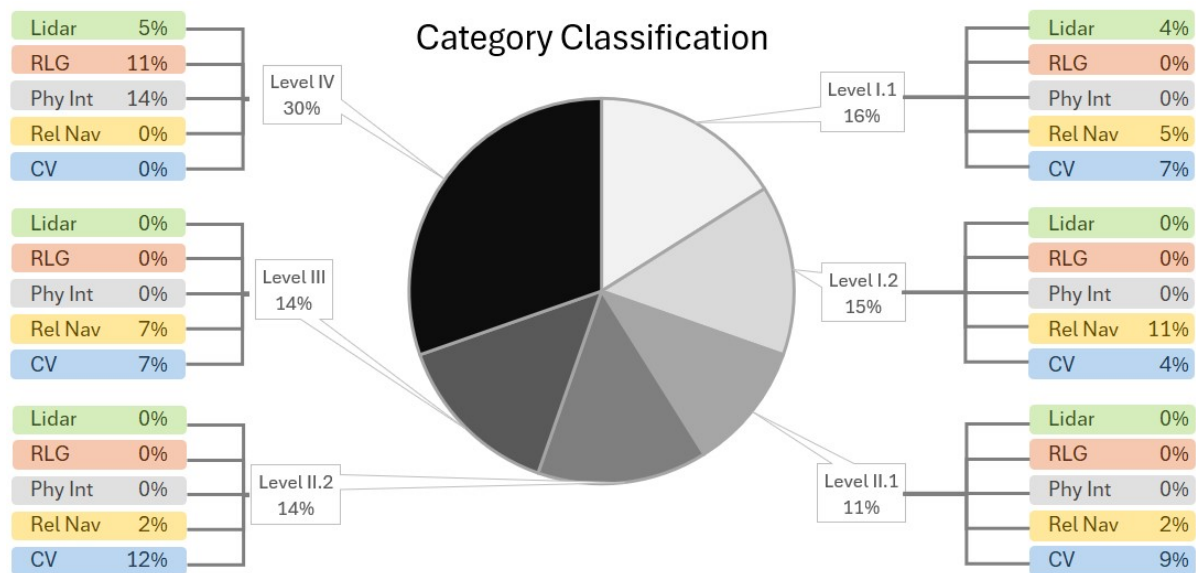


Fig. 7 Distribution of Autonomous Landing solutions by category.

legged system with joint actuation installed on a Hughes OH-6A helicopter. A state machine control sets the leg damping to nominal values once the four legs touched the ground. A PD controller with joint moment actuators was designed to level the aircraft based on attitude and rate feedback. Further investigations introduced a Virtual Mode Control (VMC) strategy simulating landings on a vessel under SS 6 [34]. The controller's goal is to maintain zero attitude and roll regardless of ship motion. Additional research [35] provided results comparing this four-legged RLG with the conventional skid configuration during a hard landing. The study demonstrated that RLG design reduces up to 90% of force and acceleration peaks. A proof of concept was carried out on a helicopter UAV [36]. A force feedback control was designed using a resistive film sensor on each foot. Each leg included two joints with angle encoders and drive systems. The controller was independent of the UAV flight computer and included its own avionics bay with IMU. Two challenges were identified: a significant payload decrease, and lack of reliable force sensors since calibration was required before each flight. A four-legged RLG system with linear actuators was also studied in [37] with a helicopter UAV (78 kg). The RLG system operates independently with its own IMU, processing unit and electric motors attached to each leg. Moreover, it did not require additional sensors since the force control was done by measuring the motor-induced currents. Experiments were limited to slope landing, but the research also introduced a scaling study which included a AS332 Super Puma (9 ton class) and a UAV Skeldar V-200 (235 kg class) helicopters.

Even with theoretical optimization, the weight increase could go up to 32.6% when compared to traditional skid [33]. The most complete investigation was done with a novel four-bar two-leg RLG system with a shared cable-driven actuator [15, 38, 39]. The authors provide insights into the design, manufacturing, and laboratory tests that resulted in an enhanced crashworthiness configuration for a 200 kg S-100 RUAV. Further research resulted in additional ground and flight tests landing on inclined terrain [40]. This study concluded that traditional force sensors were not suitable for RLG operational specifications: low force sensitivity while being capable of enduring frequent heavy loads without requiring recalibration or replacement. Therefore, a novel force sensor was developed to meet these requirements. Also, the solution included a novel PD controller that uses information from the force, aircraft roll, and leg angle sensors. This approach provided better results when compared to traditional PBC (Park Braking Control). Landing on a moving platform was investigated in rotor-off laboratory tests under scenarios up to SS 5 [41]. Further investigations were performed with multi-body simulations up to SS 6 and concluded that the novel controller presented a better performance when compared to only force feedback control and traditional skids regarding dynamic rollover avoidance. The authors acknowledge that further investigation is required by introducing ship wake and gust interference, especially in lower

collective conditions after landing. Fig. 8 provides an overview of the strategies adopted by each RLG research.

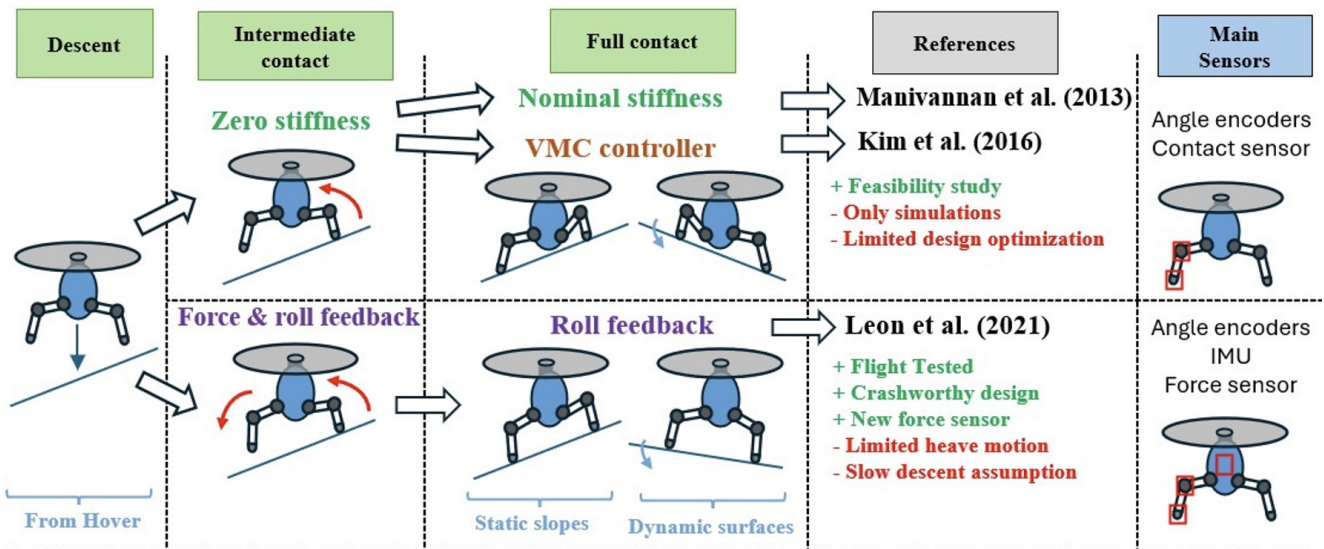


Fig. 8 Summary of main RLG strategies.

3.2 LiDAR-based Landing Systems

LiDAR-based solutions are extensively being explored for safe autonomous landing on unprepared sites [42]. This approach was also considered for pose estimation in autonomous landing on ships. Theoretically, these sensors could deliver accurate results across a range of lighting conditions. On the other hand, LiDAR performance can be jeopardized by adverse weather conditions that result in light scattering and occlusion, such as fog and rain [43].

In [44] authors developed a scanning LRF system, however, tests were limited to helicopter relative states estimation to a fixed ground position. While displaying promising results, one of the shortcomings was the limited range (16,5 m) due to power restrictions. A system that combined LiDAR and visual solutions for tracking the ship deck was developed in [45]. A higher operational range was achieved by increasing the mass and dimension of the sensor. Simulations of a 6 DoF deck sinusoidal motion demonstrated an average orientation error of 1° after applying a particle filter. The LiDAR vertical FoV was controlled to ensure continuous focus on the landing pad. This system was subsequently installed and flight-tested on a Bell 206 helicopter to detect a fixed landing pad. Another disadvantage was that minor deviations in LiDAR pointing angle could result in failing to detect the landing platform.

Autonomous landing simulations based on LiDAR pose estimation were investigated in [46]. Safe landing windows were predicted based on the forecasted pitch and roll ship motion by an FFT prediction model with discrete KF amplitude and phase estimation. The prediction time is set to 5 s, but decreases based on the estimated landing time. Overall, this approach led to fewer landing attempts but required tuning parameters a priori. Investigations were performed in high sea state conditions and included a Gaussian sensor noise based on LiDAR accuracy. The authors added two novel controls: an Active Heave Compensation (AHC) to avoid ship collision while in low hover, and a Landing Period Indicator (LPI) to estimate safe landing windows based on ship energy parameters. The combined solution successfully landed the UAV in 88% of the test scenarios, which included SS 6. Nevertheless, the results were limited to scenarios based on simulations since it was a proof of concept, and the authors recommended laboratory tests for future investigations. More recent research proposed a dual-channel LiDAR for multipurpose missions that included ship landing [47]. Simulations provided target estimation errors of -7.2° in pitch and -2.8° in roll. Initial flight tests with a small-scale water target were performed to check the accuracy

of pose estimation. Since the research focused on sensor development, no autonomous landing solution was investigated.

3.3 External Relative Navigation

Landing strategies based on relative navigation sensors were already flight-tested and deployed on operational missions [3]. Researchers successfully explored GNC solutions that track the filtered ship's position in order to maintain a prescribed height over the deck and then proceed to land as required. Overall, this standard approach provides a safe landing with good accuracy in moderate sea conditions [3, 26, 48]. Usually, the landing criteria do not take into account unsafe conditions due to ship oscillations. However, in adverse sea states, one of the challenges is how to use ship pose estimation to prescribe safe landing windows [49, 50].

The RTK-GNSS solution presented in [26] covered conditions up to SS 2 in real-scenario shipboard operation. It was the first time a tilt-rotor UAV performed automatic take-off and landing from a ship. The research demonstrated that a higher hover position was required to overcome the turbulence from the vessel. At the lower position, the UAV experienced higher performance degradation than the simulation results. Moreover, the authors explored a laterally offset hover in the landing procedure. The landing system based on RTK-GNSS was able to achieve a Circular Error Probability (CEP) lower than 2 m. On the other hand, it is still required that an operator command the landing and take-off procedures.

In [48, 51] authors explored a solution based on EKF from both RTK-GNSS data and UWB relative positioning system (50-60 m range) for a hybrid VTOL UAV. The ship speed, heading, and position were estimated by the UAV on-board computer due to limitations on the transmission rate (2 Hz) with the hardware installed on the ship. The turbulence also played a key role in both take-off and landing performance. Given the studied UAV design, the authors suggested that the highest rate of climb should be performed during take-off in order to minimize the time in turbulent ship wake. On the other hand, the authors suggested that other landing techniques such as capturing net should be explored for harsh wind conditions. In that case, the criteria to perform the autonomous landing is based on a time threshold while in the hover position.

In [49] authors explored a novel reference trajectory and robust control strategy with a relative navigation based on UWB sensors (20 cm level of accuracy). This configuration assumes that landing platform Euler angles and their rates are computed with external hardware and shared with the UAV. A high-order polynomial altitude reference trajectory is computed, and the landing criteria are based on conditions computed from estimated ship states. These conditions also rely on experimentally tuned thresholds, and the UAV would only perform the reference trajectory if these conditions are met. Flight tests were performed with a robust hierarchical control that includes trajectory tracking based on a force controller, and attitude tracking through an attitude-constrained torque controller. Lower transient errors and precise landings were achieved when compared to traditional PID controllers.

In [31] pose estimation is performed with an array of acoustic sensors. The main reason for that choice over traditional vision strategies is that authors considered Arctic missions, therefore with limited light conditions. Since relative acceleration is obtained from IMU installed on both UAV and ship, pose was computed using EKF based on a particle kinematic model and acoustic measurements. The guidance algorithm was based on a potential field approach, that provided generalized velocities. A MLP NN algorithm was developed to find safe landing windows based on forecasted ship attitudes. The landing criteria take thresholds on ship pitch and roll into account, and this approach was considered for high sea state conditions (scenarios with ship attitudes above 5° and high frequency). Overall, the results achieved a landing precision of up to 14 cm. Additionally, while using a 5s window predictor, the algorithm was able to accurately forecast safe conditions 88% of the time [50].

New approaches with MPC were investigated in [52, 53] for real-time applications. The test scenario considers a GNC solution to land a UAV on a moving USV, considering both autonomous agents. The proposed MPC architecture is based on vertical and horizontal decoupling so that the optimization can become tractable for long horizons. Regarding USV heave motion, the optimization finds the time-optimal trajectory with soft touchdown constraints instead of tracking the vertical motion. The heave motion was forecasted using a single sinusoidal FFT model from USV IMU measurements.

3.4 Physical Interfaces

Tether is one of the possible physical interfaces that enable shipboard landing. In [54, 55], the authors presented the first controller concept for a tethered small-scale UAV helicopter. Pose estimation conceptually required hardware on ship including the cable angle sensors. The controller is based on feedback linearization of a simplified helicopter model with time scale separation between rotational and translational dynamics. Assumptions included negligible cable weight and elastic effects. At close range, the attitude-altitude control goal was to follow the ship's attitudes. Results demonstrated that high cable tension decreased translational tracking error. A more detailed helicopter dynamics which included flapping dynamics was investigated in [56] with a backstepping tether control.

Experimental trials for helicopter UAV tethered guided landing without GPS assistance started with [57] [58]. This research assumed that the pitch and roll motion are actively stabilized on the ship, which is a simplified approach considering the real scenarios. Therefore, the tether system would compensate for ship heave motion. Since this first approach focused on the design of the tether control, the experimental setup was limited to landing the helicopter on a non-dynamic surface. The system included a LiDAR for precise height measurement and a ball-joint tether connection with a load sensor and angle encoder. Additionally, a reeling mechanism controls cable load via proportional gain scheduled based on tether length. A similar design was explored in [59] with the winch mechanism installed on the platform. This was the first tether experiment results that considered a moving platform with ship-simulated motion.

In [60] authors designed an electromagnetic winch tether system with the reel controller aboard the UAV. The initial design weighed 3.5 kg including 3-axis cable load and angle sensors, but the integrated solution also relies on GNSS. An improved winch prototype was flight tested and results presented a good match between GPS altitude and tether length [61]. However, landing trials were performed only on stationary targets. Another research that explored a similar design was [62]: a magnetic catcher was lowered to attach to a custom landing pad that has an interface alignment system for precise landing. Outdoor flight tests were performed on a multiple-UAV landing platform over water undergoing attitude and translational disturbances [63].

Physical interfaces with robot manipulators were also investigated as a solution for landing on ships [64–66]. Overall, the procedure is divided into three steps: approach, in-flight capturing, and coordinated touch-down. In [64] the research focused on the development of control strategies for the last phase, therefore it was assumed that the UAV was already attached to the robot manipulator interface through a universal hinge (ball joint). An active thrust control was developed in order to minimize UAV disturbances in the robot manipulator while coping with the joint torque limits. The authors simulated a common tuned control with different VTOL UAVs. However, one limitation is that the manipulator control requires UAV states and torques computed by the attitude controller. Moreover, joint torque limit was reached while performing simulations with the heaviest UAV in sea states 4 and 5. In [66] address the problem of landing the UAV on a small-scale USV. Due to high-frequency disturbances, this scenario poses additional challenges to the manipulator compared to full-scale ships, given joint constraints and bandwidth limitations. The authors developed a three-layer MPC controller based on a modified wavelet NN for wave motion prediction. The manipulator rotational and positional trajectory presented improved accuracy compared to traditional Inverse Kinematic controllers when subjected to sea wave disturbances,

but no tests were performed with UAVs. Overall, one of the shortcomings of the robot manipulator strategy is the complex hardware requirement installed on the landing platform.

3.5 Computer Vision Systems

Vision-based solutions have been widely researched in the past decade for landing on moving targets [2]. However, many researches mainly focus on ground-moving targets with limited motion that usually does not include pitch, roll, and heave oscillations. In [16], the authors listed the research progress on autonomous landing on ship-based platforms based on image processing strategies. One key challenge, however, is to enhance the robustness of optical solutions when operating in the wide range of weather conditions such as the one experienced during shipboard missions. For instance, water mist and poor lighting conditions can jeopardize the system's performance on detecting features.

In [67] authors studied time-optimal solutions for autonomous landing on heaving platforms considering only UAV acceleration and relative position as available data. The relative height was measured by a motion capture system, however, the authors further integrated a CV approach based on April Tag board detection [68]. An Adaptive Robust Control was designed to perform the trajectory tracking while performing an online estimation of the ground effect. The time optimal trajectory was computed using a bang-bang type control law. The authors assumed that the platform was undergoing a sinusoidal motion with slowly time-varying parameters to simplify the motion forecast inside the trajectory generation algorithm. The estimation module computed UAV and platform states through a standard UKF algorithm. A faster rate of convergence was achieved when compared to optical flow solutions [69].

The authors also studied a more complex scenario, including pitch motion of the platform, but limited to a 2D quadrotor model (longitudinal and vertical axes)[70]. The inner loop was designed with standard LQR feedback and MRAC (Model Reference Adaptive Control) feedforward controllers. The NP problem was reformulated to tackle terminal and collision avoidance time-varying constraints by using segment discretization based on fixed time intervals instead of fixed trajectory length discretization. It was assumed, however, that the platform motion is known. Experimental validation included UAV landing on a platform with heave and pitch motion. Successful landing was achieved in simulations considering uncertainties on target translational motion, but assumes constant speed during the prediction steps.

A low-cost experimental setup and a simple control solution were developed in [7] and tested with a custom scaled-down motion platform. A discrete-time PID control law was designed for the approach procedure based on the heading angle and horizontal distance while considering FoV limitations in the heave controller. In the second stage, while in hover, the high contrast H landing mark was detected with a monocular camera using contour extraction and comparison with a standard image. This algorithm was tested against different lighting conditions, camera resolutions, and orientations. UAV state estimation is performed with KF based on IMU data and image pose, and validated with a motion capture system. A linear altitude trajectory planner was applied to control the vertical speed during landing. Landing criteria takes into account heading and desired horizontal position errors.

An optical guidance solution was flight tested on MQ-8C Fire Scout UAV [3] as a backup system for its legacy system. The landing procedure includes high (30 ft) and low (15 ft) hover positions above the estimated TDP (Touch Down Point). The legacy system is a pulse radar relative navigation hardware which also includes an IMU installed on the ship. The estimated TDP and UAV relative position is computed on the ship hardware and sent through data link communication. On the other hand, the optical landing system performs pose estimation based only on deck pattern markings. This system includes three cameras to maximize FoV during the whole landing procedure. The authors mentioned without further details that a filter is applied to distinguish ship steady-state translation (stabilized deck frame) from its oscillation. Initial results demonstrated that the optical solution provided similar performance as the legacy system when estimating the TDP (Touch-down point) position. The deviations were limited to 2° of heading and 3 ft in TDP position in all axes.

A different approach regarding visual cues was explored by [71–73]. The idea is to use the gyro-stabilized horizon bar as a reference for pose estimation. A COTS Parrot Anafi quadcopter with a single monocular camera was flight tested lading on a 6 DOF Stewart platform with up to 17.5 kt of wind disturbance. Long-range control was based on YoLov3 ML object detection with nonlinear exponential gains to overcome the processing delay. A single-state KF was also introduced to yaw angle estimation due to noise at long distances. Close-range included Classical CV (HSV filtering, Forstner sub-pixel corner detection, and a screening algorithm for false detections) for pose estimation. A probabilistic derivative controller that also included PI feedback was developed to avoid abrupt large inputs due to eventual inaccuracies from pose estimation. The probabilistic nonlinear gain was obtained by a normal distribution with empirically tuned parameters based on aircraft movements. The UAV proceeded to land if it was inside a predefined spatial threshold that took into account the landing pad and UAV dimensions.

State-of-the-art MPC controllers for autonomous helicopter landing on ships were studied in [74, 75]. Simulations were performed with a helicopter and ship models. First, it was demonstrated that the fixed prediction horizon MPC (FH-MPC) approach was not able to handle sudden changes in ship motion, and not all final states were safely tracked [74]. Therefore, a novel MPC approach based on shrinking PH (SH-MPC) was suggested in [75]. Safe landings were achieved under ship airwake turbulence (CETI approach), model parametric uncertainties, and control constraints. The solution feasibility relies on the prescribed maneuver time defined by the user. Since it is a proof of concept, no flight tests were performed and the code performance was not optimized for embedded applications. Moreover, it does not address how ship states would be shared with the UAV. A Variable Horizon approach (VH-MPC) was also suggested in [76], also limited to simulation results.

In [77] authors presented a practical solution with a novel MPC nonlinear estimator (MPC-NE) implementation with pose estimation of fiducial tags. The studied scenario included UAV landing on a small tilting USV (pitch and roll) in rough sea states (up to 17° amplitude and 7 m/s wind disturbance). For The MPC design, it was assumed that the USV experienced minimal horizontal and heave motions. The USV motion forecast was modeled with an FFT formulation similar to [46]. Phase and amplitude were updated with a Kalman observer, assuming that modes did not change until the next FFT sampling time. Flight tests demonstrated that robust predictions were achieved between 0.25 and 0.5s. The UAV prediction model consisted of an Euler approximation of a set of single-particle kinematics. The authors included a novel MPC landing cost function that relies on USV pitch and roll as well as relative height. The cost function was activated based on thresholds on FFT accuracy, x and y position errors, and UAV horizontal speeds. During flight tests, safe landings were achieved within 50 s while USV tilting angles were less than 5°. Simulation results showed that MPC-NE achieved 94% landings within 10° against 71% of SH-MPC while requiring 9 times less computational cost.

In [78] a feed-forward term based on the estimated ship speed was introduced in the tracking controller to overcome the assumption of stationary target in standard IBVS architecture. The target states were estimated through an EKF with ship GPS data, target detection pose, and UAV states. The ship is assumed to be moving with nearly constant translational speed and has two nested Aruco landing marks. An offset is added to the rendezvous reference position to guarantee that the visual marker on the deck will be inside the camera FoV even under GPS bias and nonzero UAV attitudes. During the rendezvous stage, the camera retreat is avoided by computing an initial heading correction before the FF-IBVS is activated. The IBVS controller is designed in two-stages to track a high and then a low height above the platform. The landing criteria rely on thresholds of the IBVS positioning errors and the relative angle between the Aruco normal vector and the camera z axis.

A similar control architecture was developed in [79]. Ship states were estimated using KF and a track-to-track fusion algorithm using data from ship GNSS and the relative pose from the onboard camera. The ship motion is simplified as a constant crackle model since it is assumed that the dynamics are not known a priori. Two UAV sensor configurations were studied: fixed downward-facing camera with and

without gimbals. A virtual image plane transformation was computed when camera gimbals were not installed. The platform was designed with a three-level AR tags scheme to perform feature detection. The IBVS controller includes adaptive gain for the altitude rate to overcome losing image features due to camera FOV restriction. Moreover, unnecessary control inputs due to landing pad oscillation were eliminated with a square fitting compensation of the four ARtags.

In [80] flight tests were performed to evaluate a real-time trajectory planning algorithm based on quadratic programming (QP). An Explicit Model Following position controller was implemented with a Froude scaling approach based on the weight ratio to the full-scale reference helicopter. This scaling strategy was suggested to compute the appropriate model-scale control bandwidths. The authors successfully tested a UKF vision pose estimation, but a motion capture system was used due to UAV hardware computational limitations [81]. The USV motion was predicted with an autoregressive (AR) time series model, with reliable results up to 1.5s. A novel PH update law based on deck states was suggested, which was performed near the end of the estimated landing time. The initial PH was computed based on the relative distance between USV and UAV and maximum acceleration limits. The PH update was allowed only within a specific time window before landing. The upper time limit was defined based on the AR accuracy, and the lower limit was set to avoid sudden trajectory changes that the UAV dynamics is able to track. The new PH was selected based on a cost function that takes into account ship roll, pitch, heave, and the magnitude of change on the PH (to avoid increasing the time without penalties). Overall, flight test results demonstrated that the QP algorithm was able to match position and velocity states. On the other hand, poor performance (landing while the USV heave speed or attitudes were high) was detected whenever the PH was decreased.

4 Discussion

An overview of the screened publication database is presented in Table A1 describing the landing pad setup and providing key test features. In general, publications that addressed the landing procedure on large-scale vessels rely on a diverse set of assumptions concerning platform motion fidelity. Nevertheless, one common feature within flight-tested solutions is that DoF limitation is due to hardware setup. As an example, Fig. 3 indicates that proper heave motion would require up to 7 m travel range under SS 6. Some research propose scaling-down oscillations [7, 71, 78, 79] or simplified equivalent motion based on modal analysis [82, 83]. However, there is no common framework to perform ship down scaling, which can potentially yield unrealistic motion [84]. As a result, no research within the database covered flight tests under fully representative harsh sea state conditions (SS 5 and above) considering full-scale ships. Therefore, to expand results up to heavier class UAV, the UAV Froude model scaling (as proposed in [80]) combined with suitable down scaling procedure for ship motion can still be regarded as an open challenge.

The classification based on procedure (Vertical Approach or Direct Approach) and path planning strategy is shown in Fig 9. New research taking into account DA with Model Predictive Control (MPC) techniques has been showcased in recent publications, demonstrating contributions both through computer simulations [74, 75] and real-world flight experiments [53, 80]. While simulation results assume unconstrained computational power and precise target pose, the flight-tested approaches provided a cost-efficient optimization for embedded systems. Although small and medium-sized naval platforms may benefit from Direct Approach (DA) path planning [53], it is worth highlighting that its feasibility under operational safety constraints remains a challenge for larger UAVs, such as the MQ-8C [3]. As presented in Fig. 2, all standard procedures are still tied to the vertical path approach, even in scenarios with degraded hover performance (e.g. single-engine emergency). Moreover, during DA, FoV restrictions may also jeopardize target pose data and this was not covered in the literature that considers CV interface. On the other hand, [77] presents a novel strategy that relies on barrier functions within the cost computation while performing a Vertical Approach (VA).

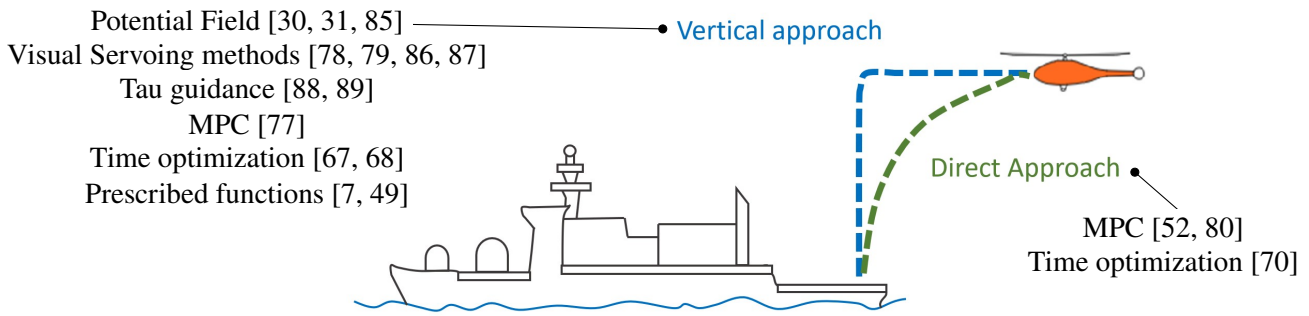


Fig. 9 Classification by path planning and procedure approach.

A performance comparison is displayed in Table 3 taking into account publications with available flight test results. The GNC strategy and landing criteria are further detailed, along with the main contributions and limitations. It should be noted that not all publications classified as Category I or II provided their performance results. While achieving a high level of accuracy, most publications do not consider landing pad attitudes inside the landing criteria. Moreover, there is no solution within the categories that included roll and heave oscillations into the landing criteria (Categories I.1 and II.1) that were tested under SS 5 or higher. Within this group, only [77] presented promising results without additional HW installed on deck for pose estimation. On the other hand, in addition to the installation of sensors, [31] is the only solution that covers the visibility constraint.

As shown in Table A1, LiDAR emerges as the sole pose estimation approach without a flight-tested solution integrated with autonomous landing GNC. Recent advancements in sensor designs are detailed in [47], alongside promising simulation results considering sensor noise [46]. On the other hand, Table A1 also illustrates a diverse array of CV strategies in recent literature. These solutions are coupled with tracking controllers such as FF-IBVS [78, 79] and PID-based alternatives [7, 71], in addition to path planning techniques like MPC [77, 80], time-optimal trajectory generation [70], and tau-guidance [88, 89].

On complex tracking scenarios, FF-IBVS approaches, as highlighted in [78, 79], still require data from a relative navigation system. While the linear velocity-free strategy [87] has shown promising simulation results, but without flight test validation in the literature. Meanwhile, despite the flexibility offered by MPC strategies in defining additional terminal safety constraints, as noted by [80], direct approach optimization strategies continue to face safety issues, particularly in scenarios with poor target state prediction. Unlike other MPC-based publications [53, 80], good landing performance was achieved in [77] by introducing a novel barrier term within the cost function with VA procedure.

Modern tether solutions achieved 90% of landing success with a robust control approach [59], and promising designs are being developed to minimize the ship hardware requirement [61]. However, when considering harsh sea states, there is room for improvements that are not limited to compensating heave oscillations but also targeting roll motion. Moreover, the attachment phase remains an open challenge with no published feasibility study. This procedure can be considered critical due to undesired cable oscillations, especially in turbulent ship air wakes and rotorcraft downwash. Failsafe designs also need to be addressed from an airworthiness perspective, along that would require extensive validation conditions due to rotorcraft flight controller modifications. Additionally, on the interface compensation approach, robot assistance provides a solution that can potentially cover a wide range of rotorcraft without requiring significant changes on the UAV side [64, 66]. While suitable for low-scale platforms, complex hardware is one of the major drawbacks to scale up to shipboard operations.

Table 3 Performance comparison of main flight tested solutions.

Ref	Weight	Metrics	DoF	Cat	Pr	GNC and landing criteria	Contributions	Limitations
[31]	700 g	MLE < 14 cm	4 SH PR	I.1	VA	Close range solution based on acoustic sensors. PID tracking with a potential field for height state. Target pitch and roll are forecasted with NN. Landing criteria: attitudes lower than 5°. SS 3 (different wave directions) with 10 m/s ship speed. Indoor test.	Acoustic positioning enhances operation under no visibility conditions. Sea state predictor for appropriate landing window.	No harsh sea state. Relies on HW on deck (acoustic sensors).
[77]	4.5 kg	Landed < 5°	3 H PR	I.1	VA	Path planning based on MPC-NE. Landing criteria based on forecasted target states (FFT + KF) with novel cost optimization with barrier function. SS 6 with tilt up to 17°, outdoor test with wind disturbances.	Implementation of MPC-NE. Higher landing success (compared to SH-MPC). No HW on deck.	FT with limited heave motion. No available MLE data.
[80]	3 kg	MLE < 30 cm	6 SSwH PYR	I.1	DA	MPC path planning with EMF tracking controller. Optimization included terminal cost. Preassigned landing time-based on tau guidance, PH update based on forecasted states (AR model)	Froude model scaling methodology. Extensive FT results under a wide range of oscillations.	Some unsafe landings (poor forecast and PH dynamic decrease).
[79]	5 kg	MLE < 30 cm	6 SSwH PYR	II.1	VA	Close range solution based on FF-IBVS. Up to SS 4 and ship speed up to 6 m/s. Outdoor test. Landing criteria based on image feature errors (indirectly related to pad attitudes and position).	Adaptive gain for FoV restrictions and square compensation to avoid oscillations.	Relies on GNSS.
[78]	3.3 kg	MLE < 5,5 cm	3 H PR	II.1	VA	PID tracking and FF-IBVS with saturation function. Tilt up to 10° and 30 cm in heave (0.2 Hz), outdoor tests with wind disturbances. Landing threshold based on attitudes, height, and image plane errors.	Extensive outdoor testing with FF-IBVS.	Manual oscillation input with no fidelity comparison. Relies on GNSS.
[49]	1.1 kg	MLE < 88 cm	4 SH PR	II.1	VA	Hierarchical tracking control with prescribed altitude path planning (high order polynomials). SS 4 with 10 km/h and SS 2 with 20 km/h. Outdoor test. Experimentally tuned landing criteria also based on rates.	High fidelity motion platform. Results outperformed traditional PID tracking controller.	Requires HW on deck (UWB anchors) and GNSS.
[7]	400 g	MLE < 14 cm	3 H PR	II.2	VA	Long-range tracking PID control with IR detection. Close-range PID tracking based on CV pose estimation (H landing mark). Path planning is based on a prescribed linear function.	Robust pose estimation in broad light conditions. No wind disturbances.	Heave fidelity. No attitude criteria. HW on deck (IR beacons).
[71]	250 g	MLE < 14 cm	6 SSwH PYR	II.2	VA	ML long-range tracking. Close-range tracking with probabilistic nonlinear control. SS 6 and 4.5 m/s ship speed. Outdoor test with up to 9 m/s wind. Landing criteria based on spatial threshold.	Extensive outdoor testing. Gyro-stabilized bar CV reference approach. No HW on deck.	Limited heave motion. No attitude criteria.
[90]	0.5 kg	MLE < 21 cm	3 - SSwH	II.2	VA	UDE-based controller for relative position and PI for relative heading. Indoor test with wind disturbances. Up to SS 4.	Enhanced tracking under external disturbances (compared to optical flow control). No HW on deck.	No attitude criteria.
[85]	Light	MLE < 12 cm	3 H PR	II.2	VA	PID tracking controller with repulsive force path planning (cone restriction above the landing pad). Vehicle speed of 4 mph with 10° pitch and roll oscillations (3 s period)	Experimental results with precise landing performance.	HW on deck (RTK-GNSS and IMU). No attitude criteria.
[59]	15 kg	90% suc- cess rate	3 SH Y	IV	VA	Tether control with cable angle and tension sensors, up to SS 5, ship speed up to 10 m/s. Outdoor test. Landing criteria does not take into account landing pad attitudes.	First flight test of tether control. No GNSS. Alternative solution with low visibility.	Attachment phase not addressed. UAV limitation to compensate large accelerations.

The safe landing algorithms rely on pose estimation and motion prediction accuracy. Short-term prediction included algorithms based on Minor Component Analysis (MCA) [76], FFT [46, 52, 77], AR models [80] and learning approaches [31], which overall include prediction windows from 0.5 to 5.0 s. There are, however, some exceptions in the Level I group that use current ship states based on FF-IBVS [49, 78] and hierarchical approach [79]. LiDAR and CV approaches do require minimal or even no hardware requirements on the landing platform. For instance, in principle no additional visual cues were required in [3, 71] since the pose estimation is based on helipad marks and the gyro-stabilized horizon bar. As mentioned, besides the high landing accuracy as per Table 3, not all landing attempts fall within the safety constraints of the landing criteria [46, 77, 80].

The Robotic Landing Gear (RLG) solutions have demonstrated promising results in both flight tests and simulations, effectively avoiding dynamic rollovers under challenging sea conditions [41]. However, two primary challenges persist: weight optimization and ensuring airworthiness. In their study, [39] developed a crashworthy design integrating ground resonance analysis and drop tests. A notable contribution lies in the development of a novel force sensor capable of withstanding continuous landing operations, which can provide reliable data to the landing controller. Moreover, the authors incorporated rotor thrust dynamics, enabling a more comprehensive analysis of the delay in reducing thrust, which increases the risk of rollover. As mentioned by the authors, the novel roll and force feedback controller does not offer short-term benefits during landing due to limitations in actuators, which could jeopardize performance in high-rate descent landings, such as those in harsh sea state conditions when a proper landing window is identified. Given that the latest RLG publications generally lack integration with the rotorcraft GNC, additional investigations could be performed to determine whether previous data from target pose estimation and forecasting models could improve landing performance in high sea state (SS) conditions. Moreover, future improvements include fault-tolerant and failsafe designs from a robustness perspective.

Despite the promising results, weight optimization remains a significant challenge for innovative landing gear designs, particularly regarding their scalability to heavier class UAVs. Table 4 provides a summary comparison of design penalties and additional capabilities of current literature designs, which have either undergone flight tests or are theoretically based on previously tested concepts.


Table 4 Comparison of RLG solutions

Rotorcraft	Analysis	Original EW (kg)	RLG Legs	Design penalties		Additional capabilities		Refs
				Weight	Payload	Slope landing envelope (roll)	Landing on dynamic surface	
S-100 Camcopter	FT, GT and SIM	110	2	+12 kg (+11%)	-24%	Up to 15° @ 98 ft/min	Avoided dynamic rollover up to SS 6	[15, 39, 41]
Rotor Buzz	FT	68	4	+ 19 kg (+28%)	-50%	Up to 30°	Not evaluated	[36, 91]
Scout B1-100	FT	60	4	+ 12,5 kg (+21%)	-70%	Up to 25°	Not evaluated	[37]
Skeldar V-200	Theoretical	195	4	+ 27 kg (+14%)	-68%	Increased by 19°	Not evaluated	[37]
Airbus AS-332	Theoretical	6.000	2	+ 337 kg (+6%)	-8%	Increased by 11°	Not evaluated	[37]

Novel concepts like the Campcopter RLG [41] demonstrated an approximate 24% decrease in the payload. For larger helicopters like the AS-332, theoretical optimization yielded an 8% decrease while focusing solely on slope landing scenarios [37]. Hence, another research gap is to improve the RLG design for full-scale aircraft, encompassing UAVs such as the MQ-8C [3], or as a landing assistance system for manned helicopters. Given the limited power-to-weight ratio of electric actuators, alternative

design solutions such as pneumatic or electro-hydraulic systems should be considered [41]. Instead of completely redesigning the landing gear, incorporating semi-active suspensions with variable stiffness and damping systems could provide a way to reduce weight and mitigate rollover risks during the transient phase of landing.

Finally, based on the literature survey, Fig. 10 presents a summary of the general features of each group, along with the main publications that presented results for harsh sea state conditions.









		Airworthiness & Qualification challenges	Adaptability from legacy systems	Fault tolerant & Failsafe designs	Landing pad HW changes	Most advanced solutions towards high sea state
	RLG	RLG V&V with high descent [41]	High complexity [37,41]	Fault detection only [41]	Minimal [41]	Force and roll controller - SS 6 with tilt oscillations [41]
	Tether	UAV FC V&V [57,59] (attachment phase)	Intermediate complexity [59]	Not addressed	Intermediate [59]	Tether tension controller - SS 5 with tilt oscillations [59]
	Manipulator	UAV FC V&V [62] (after capture phase)	Potentially minimal [64-66]	Not addressed	Complex [64-66]	Manipulator impedance controller - SS 6 (simulation only) [64]
	LiDAR	Adverse environment V&V	Intermediate complexity [45]	Not addressed	Minimal [45,46]	LPI, AHC and SPA - SS 6 with heave oscillations (simulation only) [46] MPC-NE - SS 6 with tilt oscillations [77]
	CV	Adverse environment V&V	Potentially minimal [3]	Usually backup of Rel Nav [3]	Minimal [3,71,77,79]	FF-IBVS - SS 4 [79] Probabilistic control - SS 6 with tilt oscillations [71]
	Rel Nav	Adverse environment V&V	Potentially minimal [19]	Not addressed	Intermediate [49]	Hierarchical control - SS 4 [49]

Fig. 10 Summary of features of each group.

5 Conclusion

This paper presents an overview of ongoing research into shipboard landing of autonomous VTOL aircraft. Database criteria included publications featuring landing targets undergoing at least roll, pitch, or heave oscillations with flight test results. To account for vessel hardware requirements, publications were classified into the following groups: Relative Navigation Systems, Computer Vision, LiDAR, Robotic Landing Gear, and Physical Interfaces (Tether and Robot assistance). A more refined classification, which considered both the autonomous level and landing criteria, provided valuable insight into the underlying approaches within each research. Besides Froude scaling techniques for control bandwidth, it was found that there is no common framework to assess scaled-down experiments, especially when it comes to platform motion fidelity. Precise landings were successfully accomplished through various methodologies; however, demonstrations were limited to low-sea-state conditions or focused on a narrow set of platform oscillations. Advanced results in high-sea-state conditions, which included MPC and FF-IBVS frameworks, either consider landing criteria that do not take into account ship states or fail to comply with safety constraints under low accuracy of pose estimation or unreliable ship motion prediction. On the other hand, RLG designs demonstrated promising results and could be explored in an integrated approach. The suggested research gaps cover challenges to scale up this solution that require minimal landing gear changes, failsafe designs, and weight optimization.

Acknowledgments

This work was supported and sponsored by MBDA UK and the Brazilian Air Force through sponsorship P20227.

Appendix

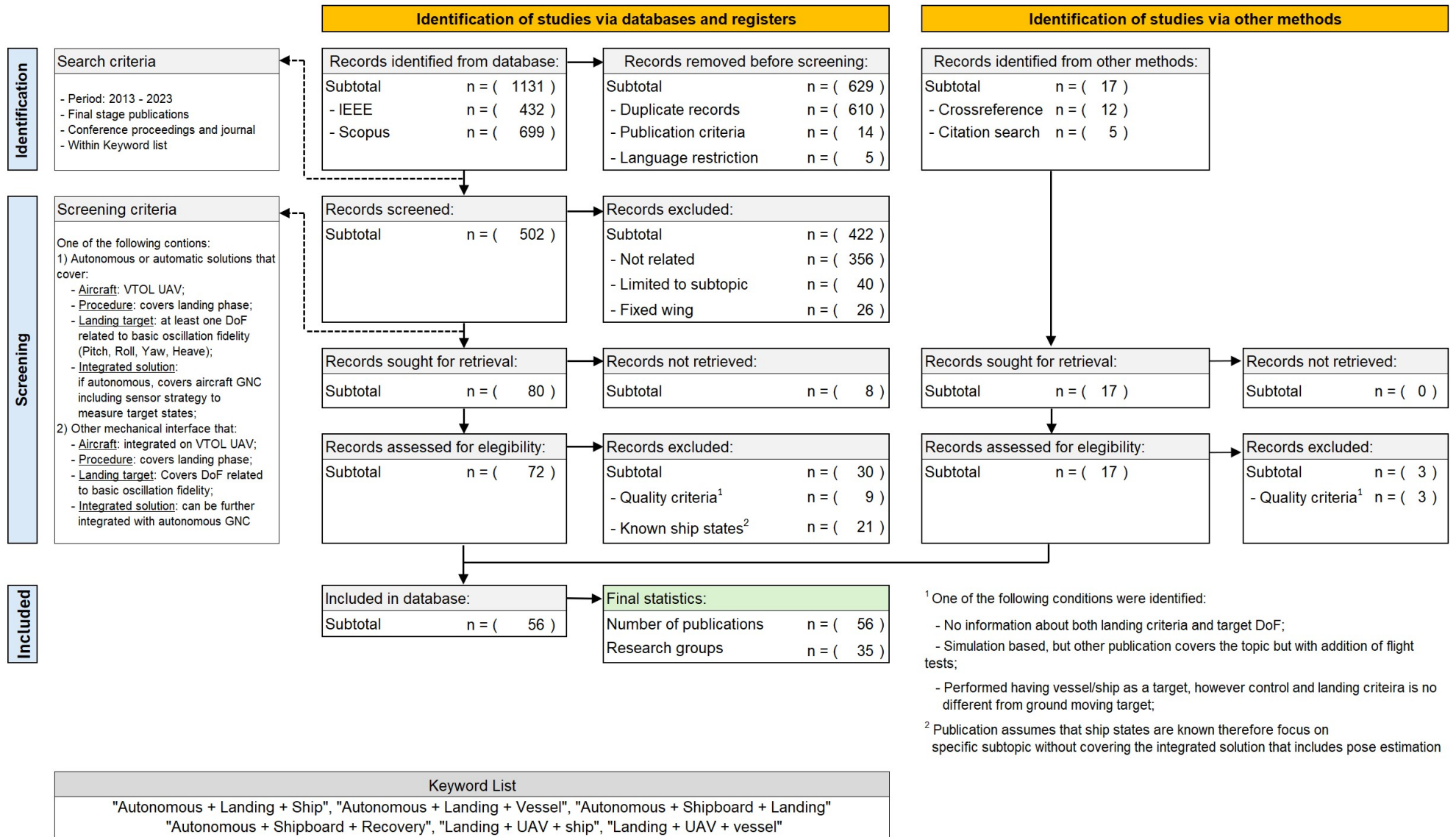


Fig. A1 PRISMA identification and screening workflow.

Table A1 Categories based on autonomous level and landing criteria

Refs	Rotor	m (kg)	Interface	Cat	DoF	Landing pad description: motion fidelity and HW requirements	Test limits and details	TRL
[45]	Heli	1500	LIDAR / CV	IV	2 (- / PR)	Simplified (GT: subscale sinusoidal motion, FT: Fixed landing pad). Landing marks.	GT: Pitch and roll rates up to 25°/s. FT: detection from 180 m away from landing pad.	GT FT
[47]	Octa	-	LIDAR	IV	6 (SSwH/PYR)	Real motion (Reduced scale landing pad). No requirements.	Relative angle and distance measurements with focus on sensor design.	FT
[46]	Quad	4	LIDAR	I.1	4 (SH/PR)	Simulated (33 m length vessel). No requirements.	Wide range of ship heading, speed up to 10 kt, up to SS 6	SIM
[41]	Heli	200	RLG	IV	5 (SSwH/PYR)	Simulated (Arleigh-Burke class vessel). No requirements.	GT: SS 5, Limited amplitude (SSwH) axes and rates up to 10°/s due to platform limits. SIM: Up to SS 6.	GT SIM
[34]	Heli	2050	RLG	IV	6 (SSwH/PYR)	Simulated (150 m length vessel). No requirements.	Up to SS 6 with 10 kt ship speed. No wind disturbances.	SIM
[61]	Heli	85	Physical: Tether	IV	0 (-)	Initial tests with docked vessel. Physical coupling hardware.	Performed attached on fixed point on ground	FT
[62]	Quad	Light	Physical: Tether	IV	1 (- /R)	Simplified (Indoor: roll sine motion, outdoor: USV free motion over water). Compatible hardware (magnetic catcher and alignment system).	Indoor: 10° roll amplitude sine waves Outdoor: USV landing platform	FT
[59]	Heli	15	Physical: Tether	IV	3 (SH/Y)	Simplified (platform attach to a vehicle with heave motion). Tether hardware and cable reel system.	Heave based on simplified wave motion and Beaufort scale, horizontal motion with compatible speed profile. Up to SS 5.	FT
[64]	Multi	0.5-44	Physical: Manipulator	IV	3 (SwH/R)	Simulated (83 m length vessel). Manipulator hardware and communication channel with UAV	Multiple types of UAV were simulated ranging from quadcopter to helicopters. Up to SS 5.	SIM
[66]	Quad	Light	Physical: Manipulator	IV	2 (- /PR)	Real (recorded USV data). Manipulator hardware	Up to 1 Hz and 10° of pitch and roll motion.	SIM
[26]	Tilt	200	RelNav: GNSS/UWB	III	6 (SSwH/PYR)	Real (Full-scale 100 m length vessel). RTK-GNSS, IMU and datalink.	Up to SS 2 with 10 kt ship speed. First automatic take-off and landing tiltrotor shipboard operation.	FT
[51]	Hyb	20	RelNav: GNSS/UWB	III	6 (SSwH/PYR)	Real (Full-scale 189 m length vessel). Relative UWB navigation station and datalink.	0-13 m/s wind gusts, 6 - 8 m/s relative wind, 13 kt ship speed	FT
[85]	Quad	Light	RelNav: RTK-GNSS	II.2	3 (H/PR)	Simulated. Sway platform attached to a vehicle with RTK-GNSS system.	Specified output values of ship motion, but achieved through manual inputs.	FT

Table A1 Categories based on autonomous level and landing criteria (continued)

Refs	Rotor	m (kg)	Interface	Cat	DoF	Landing pad description: motion fidelity and HW requirements	Test limits and details	TRL
[52]	Quad	2.4	RelNav: GNSS	I.2	3 (SH/Y)	Simulated (nonlinear ground vehicle model with single sinusoidal heave motion). Processed IMU and GNSS data sent to UAV.	Experiments only with virtual simulated boat. IMU and GPS data (added noise) with up to 3 m/s ship speed. Moderately windy conditions.	FT
[70]	Quad	1	RelNav: MC	I.2	2 (H/P)	Simplified (prescribed sinusoidal motion). Motion capture required (Operational pose estimation was not the focus of the study).	Control covers only longitudinal and vertical axis. Prescribed sinusoidal heave and pitch motion.	FT
[49]	Quad	1.1	RelNav: UWB/DL	II.1	4 (SH/PR)	Simulated (Sway platform attached to a vehicle). GPS, IMU and UWB systems that communicate with UAV.	SS 4 with 10 km/h and SS 2 with 20 km/h, outdoor tests under wind disturbances.	FT
[31]	Quad	0.7	RelNav: Acoustic	I.1	4 (SH/PR)	Simulate (Stewart platform: simulated 112 m length vessel - HMCS Nipigon). Acoustic sensors.	SS 3 with 10 m/s ship speed	FT
[80]	Quad	3	CV / RelNav: MC	I.1	5 (SSwH/PR)	Real (Downscale 20 ft length USV). Pose estimation performed with Motion capture, but initial tests performed with CV based on tags.	Three set of USV conditions which included 2.8 and 2.3 rad/s (frequency corresponding to the peak in the wave amplitude spectrum) and different headings.	FT
[3]	Heli	2700	CV	III	6 (SSwH/PYR)	Real motion (Full-scale ship USS Jackson LCS 6). Landing pattern on deck (circle, point and lines) and datalink.	Total of 78 shore and 27 shipboard approaches compared with legacy RelNav systems. Limits not mentioned.	FT
[7]	Quad	0.4	CV	II.2	3 (H/PR)	Scaled down (custom small-scale platform). 4 LEDs and H landing mark.	Equivalent to SS 6 based on the maximum pitch of the landing platform. Heave limited to 6 cm displacement.	FT
[71]	Quad	0.25	CV	II.2	6 (SSwH/PYR)	Scaled down (Stewart platform attached to vehicle). Horizontal stabilized visual cue	Up to SS 6 and 4.5 m/s ship speed with changing course. Outdoor tests with up to 9 m/s wind.	FT
[79]	Quad	5	CV / RelNav: GPS	II.1	6 (SSwH/PYR)	Scaled down (Stewart platform attached to a vehicle). Shared ship GNSS data with UAV. Three Level visual cues (AR tags).	Translation motion was 1:10 scaled down. Up to SS 4 and ship speed up to 6 m/s.	FT
[68]	Quad	Light	CV	I.2	1 (H/ -)	Simplified (Small heave platform with sinusoidal motion). April Tag pattern	Prescribed heave motion with two sinusoidal components. No wind disturbances.	FT
[78, 92]	Octa	3.3	CV / RelNav: GPS	II.1	3 (H/PR)	Scaled down (Platform attached to a vehicle with manual inputs). GPS data streamed to the UAV, two level ArUco markers.	Amplitudes up to 10° in roll, 7° in pitch, and 30 cm in heave with approximately 0,2 Hz. Outdoor tests with wind disturbances.	FT
[77]	Quad	4.5	CV	I.1	3 (H /PR)	Real motion (Custom small size USV). Fiducial tag.	FT: Wind up to 12 m/s, Wave height up to 4 m. SIM: Also covered slow drifting scenarios	FT SIM

Table A1 Categories based on autonomous level and landing criteria (continued)

Refs	Rotor	m (kg)	Interface	Cat	DoF	Landing pad description: motion fidelity and HW requirements	Test limits and details	TRL
[67]	Quad	Light	CV	I.2	1 (H)	Simplified. Small heave platform with sinusoidal motion.	Specified input of 0.1 m amplitude and 0.3 Hz.	FT
[83]	Quad	2.8	CV	III	5 (SSwH/PR)	Simulated (COTS small stewart platform). Fiducial markers.	Tests focused on pose estimation algorithm. Up to SS 6.	FT
[93]	Quad	0.9	CV	III	3 (PRY)	Simplified (Custom small scale platform). LED and ArUco markers	Sinusoidal motions with provided history plots	FT
[94]	Quad	2.7	CV	II.2	1 (H)	Simplified (Heave motion platform).IR beacons.	Prescribed heave motion.	FT
[90]	Quad	0.5	CV	II.2	3 (SSwH/-)	Simulated. SIM: Heave motion based on USS Joseph Hewes destroyer RAO FT: Custom landing pad with linear stage actuator	SIM: Up to SS 4 with 10 kt ship speed, and 19 kt average wind FT: Simplified sinusoidal motion (due to actuator limits) with fan wind disturbance	SIM FT
[87]	Heli	7.4	CV	I.1	6 (SSwH/PYR)	Simplified (Simulated based on sinusoidal inputs). Visual markers.	Deck motion is described as relatively harsh environment but not compared with sea state conditions	SIM
[86]	Quad	Light	CV	II.1	6 (SSwH/PYR)	Simplified (Custom small scale landing pad). Visual markers.	Deck motion was limited to 80 in amplitude due to hardware limitations. Investigated scenarios included oscillation periods of 1 and 2 s.	SIM FT
[88]	Hexa	Light	CV	II.1	6 (SSwH/PYR)	Simulated (Wave and vessel dynamics based on Unity 3D software)	Does not clearly specify test limits.	SIM
[95]	Quad	Light	CV / RelNav	II.1	6 (SSwH/PYR)	Simplified (Landing pad attached to 6 DoF manipulator installed on a mobile ground vehicle). Visual marker (April Tags) and ultrasonic sensors	Oscillations are simulated with Pierson-Markowitz spctrum function (considering 7 m/s wind). Frequencies between 0.4 and 1.3 Hz, wave amplitude limited to 0.5 m	FT
[89]	Tri	Light	CV	II.2	6 (SSwH/PYR)	Simplified (Small scale landing. Motion is modelled as a Gaussian noise). Visual marker (April Tags) and ultrasonic sensors	Fairly slow with pitch, surge, and sway periods of 20 s, 17s and 17s respectively. Limited to low sea states conditions.	FT

References

- [1] Syed Agha Hassnain Mohsan, Nawaf Qasem Hamood Othman, Yanlong Li, Mohammed H. Alsharif, and Muhammad Asghar Khan. Unmanned Aerial Vehicles (UAVs): Practical Aspects, Applications, Open Challenges, Security Issues, and Future Trends. *Intelligent Service Robotics*, 16(1):109 – 137, 2023. DOI: [10.1007/s11370-022-00452-4](https://doi.org/10.1007/s11370-022-00452-4).
- [2] Inderjit Chopra. Small UAS and Delivery Drones: Challenges and Opportunities the 38th Alexander A. Nikolsky Honorary Lecture. *Journal of the American Helicopter Society*, 66, 10 2021. ISSN: 00028711. DOI: [10.4050/JAHS.66.042001](https://doi.org/10.4050/JAHS.66.042001).
- [3] Doug Duehring, Brendan Egan, and Avinash Gandhe. Test and Evaluation of Image-Based Navigation for Shipboard Landing on the MQ-8C Fire Scout Unmanned Aircraft System. In *79th Annual Forum and Technology Display*. Vertical Flight Society, 2023.
- [4] Marc D. Takahashi, Matthew S. Whalley, Hossein Mansur, Carl R. Ott, Joseph S. Minor, Zachariah G. Morford, Chad L. Goerzen, and Gregory J. Schulein. Autonomous Rotorcraft Flight Control with Multilevel Pilot Interaction in Hover and Forward Flight. *Journal of the American Helicopter Society*, 62(3), 2017. DOI: [10.4050/JAHS.62.032009](https://doi.org/10.4050/JAHS.62.032009).
- [5] Mark B. Tischler. Flight Control Technology Advancements and Challenges for Future Rotorcraft 40th Alexander A. Nikolsky Honorary Lecture. *Journal of the American Helicopter Society*, 67, 10 2022. ISSN: 00028711. DOI: [10.4050/JAHS.67.041001](https://doi.org/10.4050/JAHS.67.041001).
- [6] Jiqiang Li, Guoqing Zhang, Changyan Jiang, and Weidong Zhang. A Survey of Maritime Unmanned Search System: Theory, Applications and Future Directions. *Ocean Engineering*, 285:115359, 2023. ISSN: 0029-8018. DOI: <https://doi.org/10.1016/j.oceaneng.2023.115359>.
- [7] Liyang Wang and Xiaoli Bai. Quadrotor Autonomous Approaching and Landing on a Vessel Deck. *Journal of Intelligent and Robotic Systems: Theory and Applications*, 92:125–143, 9 2018. ISSN: 15730409. DOI: [10.1007/s10846-017-0757-5](https://doi.org/10.1007/s10846-017-0757-5).
- [8] Dev Minotra and Karen M. Feigh. An Analysis of Cognitive Demands in Ship-based Helicopter-landing Maneuvers. *Journal of the American Helicopter Society*, 65, 10 2020. ISSN: 00028711. DOI: [10.4050/JAHS.65.042009](https://doi.org/10.4050/JAHS.65.042009).
- [9] R Bruce Lumsden, Colin H Wilkinson, and Gareth D Padfield. Challenges at the Helicopter-Ship Dynamic Interface. In *24th European Rotorcraft Forum*, 1998. <https://dSPACE-erf.nlr.nl/server/api/core/bitstreams/270164be-a9a3-4b06-b362-685389806311/content>.
- [10] A. Hoencamp. *Helicopter-Ship Qualification Testing*. PhD thesis, TU Delft, 2015.
- [11] Mohammed Aissi, Younes Moumen, Jamal Berrich, Toumi Bouchentouf, Mohammed Bourhaleb, and Mohammed Rahmoun. Autonomous solar USV with an automated launch and recovery system for UAV: State of the art and Design. In *2020 IEEE 2nd International Conference on Electronics, Control, Optimization and Computer Science, ICECOCS 2020*. Institute of Electrical and Electronics Engineers Inc., 12 2020. ISBN: 9781728169217. DOI: [10.1109/ICECOCS50124.2020.9314415](https://doi.org/10.1109/ICECOCS50124.2020.9314415).
- [12] Samuel S. Evans. The incredible story of the QH-50 DASH the first unmanned helicopter turns 50. *Vertiflite*, 57(1):36 – 39, 2011. Cited by: 1.
- [13] Norman Polmar. The Unmanned Helicopter. *Naval History Magazine*, 13(6), 1999.
- [14] Carlo Giorgio Grlj, Nino Krznar, and Marko Pranjić. A Decade of UAV Docking Stations: A Brief Overview of Mobile and Fixed Landing Platforms. *Drones*, 6, 1 2022. ISSN: 2504446X. DOI: [10.3390/drones6010017](https://doi.org/10.3390/drones6010017).
- [15] Benjamin León. *Enabling Technologies for Autonomous Landing with Robotic Landing Gear*. PhD thesis, Georgia Institute of Technology, 2020.

- [16] Long Xin, Zimu Tang, Weiqi Gai, and Haobo Liu. Vision-Based Autonomous Landing for the UAV: A Review. *Aerospace*, 9, 11 2022. ISSN: 22264310. DOI: [10.3390/aerospace9110634](https://doi.org/10.3390/aerospace9110634).
- [17] Alvika Gautam, P.B. Sujit, and Srikanth Saripalli. A Survey of Autonomous Landing Techniques for UAVs. In *2014 International Conference on Unmanned Aircraft Systems (ICUAS)*, pages 1210–1218, 2014. DOI: [10.1109/ICUAS.2014.6842377](https://doi.org/10.1109/ICUAS.2014.6842377).
- [18] AGARD. Helicopter/Ship Qualification Testing. Agard-ag-300 vol.22, Advisory Group for Aerospace Research and Development (AGARD), Neuilly-sur-Seine, France, 2003.
- [19] Alanna Wall, Kevin McTaggart, Eric Thornhill, Perry Comeau, Richard Lee, and Sean McTavish. Opportunities for expanding shipboard-helicopter operational envelopes using modelling and simulation tools. *STO - Meeting Proceedings Paper*, 2018. Published: 10/5/2018. DOI: [10.14339/STO-MP-MSG-159-02-PDF](https://doi.org/10.14339/STO-MP-MSG-159-02-PDF).
- [20] Helideck Certification Agency. Helideck Limitations List Part C. Internal Document, 2014. Accessed on April 17, 2024. Available upon request from the Helideck Certification Agency. <https://www.helidecks.org/wp-content/uploads/2023/07/HLL-Part-C-P-R-H-Tables-Feb-2023.pdf>.
- [21] Bochan Lee. *On the Complete Automation of Vertical Flight Aircraft Ship Landing*. PhD thesis, Texas A&M University, 2021. <https://hdl.handle.net/1969.1/195166>.
- [22] Susan L Bales. Designing Ships to the Natural Environment. Technical report, ASSOCIATION OF SCIENTISTS AND ENGINEERS OF THE NAVAL SEA SYSTEMS COMMAND, 1982.
- [23] WMO. International Codes Volume I.1 Annex II to the WMO Technical Regulations Part A – Alphanumeric Codes. Technical report, WMO - World Meteorological Organization, 2019.
- [24] NATO. Standardized Wave and Wind Environments for NATO Operational Areas. Technical report, NATO, 1983.
- [25] Thomas Rakotomamonjy and Quang Huy Truong. Helicopter Ship Landing using Visual Servoing on a Moving Platform. *IFAC-PapersOnLine*, 50:10507–10512, 7 2017. ISSN: 24058963. DOI: [10.1016/j.ifacol.2017.08.1275](https://doi.org/10.1016/j.ifacol.2017.08.1275).
- [26] Youngshin Kang, Bum Jin Park, Am Cho, Chang Sun Yoo, Yushin Kim, Seongwook Choi, Sam Ok Koo, and Soohun Oh. A Precision Landing Test on Motion Platform and Shipboard of a Tilt-Rotor UAV Based on RTK-GNSS. *International Journal of Aeronautical and Space Sciences*, 19:994–1005, 12 2018. ISSN: 20932480. DOI: [10.1007/s42405-018-0081-8](https://doi.org/10.1007/s42405-018-0081-8).
- [27] Tristán Pérez and Mogens Blanke. Simulation of ship motion in seaway. 2002. <https://api.semanticscholar.org/CorpusID:17878195>.
- [28] S Bales, W Meyers, and G Rossignol. Response Predictions of Helicopter Landing Platform for The USS Belknap (DLG-26) And USS Garcia (DE-1040)-Class Destroyers. Technical report, US Navy Ship Research and Development Center, 1973.
- [29] T Applebee and A Baitis. Response Amplitude Operator Predictions for the USS Belknap (DLG-26) And USS Joseph Hewes (DE-1052) Class Destroyers. Technical report, US Naval Ship Research and Development Center, 1974.
- [30] J. Ross, M.L. Seto, and C. Johnston. Autonomous Zero-visibility Quadrotor Landings towards Persistent Ship-based UAV Ocean Observations. In *OCEANS 2019 MTS/IEEE SEATTLE*, pages 1–6, 2019. DOI: [10.23919/OCEANS40490.2019.8962612](https://doi.org/10.23919/OCEANS40490.2019.8962612).
- [31] Jordan Ross, Mae Seto, and Clifton Johnston. Autonomous Landing of Rotary Wing Unmanned Aerial Vehicles on Underway Ships in a Sea State. *Journal of Intelligent and Robotic Systems: Theory and Applications*, 104, 1 2022. ISSN: 15730409. DOI: [10.1007/s10846-021-01515-x](https://doi.org/10.1007/s10846-021-01515-x).

- [32] Sebastian Küchler, Tobias Mahl, Jörg Neupert, K. Schneider, and Oliver Sawodny. Active Control for an Offshore Crane using Prediction of the Vessels Motion. *IEEE/ASME Transactions on Mechatronics*, 16:297–309, 4 2011. ISSN: 10834435. DOI: [10.1109/TMECH.2010.2041933](https://doi.org/10.1109/TMECH.2010.2041933).
- [33] Vasudevan Manivannan, Jared P. Langley, Mark F. Costello, and Massimo Ruzzene. Rotorcraft Slope Landings with Articulated Landing Gear. In *AIAA Atmospheric Flight Mechanics (AFM) Conference*, 2013. DOI: [10.2514/6.2013-5160](https://doi.org/10.2514/6.2013-5160).
- [34] Dooroo Kim and Mark Costello. Virtual Model Control of Rotorcraft with Articulated Landing Gear for Shipboard Landing. In *2016 AIAA Guidance, Navigation, and Control Conference*. American Institute of Aeronautics and Astronautics Inc, AIAA, 2016. ISBN: 9781624103896. DOI: [10.2514/6.2016-1863](https://doi.org/10.2514/6.2016-1863).
- [35] J. Kiefer, M. Ward, and M. Costello. Rotorcraft Hard Landing Mitigation Using Robotic Landing Gear. *Journal of Dynamic Systems, Measurement and Control, Transactions of the ASME*, 138, 3 2016. ISSN: 15289028. DOI: [10.1115/1.4032286](https://doi.org/10.1115/1.4032286).
- [36] Defense Advanced Research Projects Agency. Robotic landing gear could enable future helicopters to take off and land almost anywhere. <https://www.darpa.mil/news-events/2015-09-10>. Accessed: 2023-08-23.
- [37] Boris Stolz, Tim Brödermann, Enea Castiello, Gokula Englberger, Daniel Erne, Jan Gasser, Eric Hayoz, Stephan Müller, Lorin Mühlebach, Tobias Löw, Dominique Scheuer, Luca Vandeventer, Marko Bjelonic, Fabian Günther, Hendrik Kolvenbach, Mark Höpflinger, and Marco Hutter. An Adaptive Landing Gear for Extending the Operational Range of Helicopters. In *International Conference on Intelligent Robots and Systems (IROS)*. IEEE/RSJ, 10 2018. ISBN: 9781538680940.
- [38] Claudio V. Di Leo, Benjamin Leon, Jacob Wachlin, Martin Kurien, Julian J. Rimoli, and Mark Costello. Cable-driven four-bar link robotic landing gear mechanism: Rapid design and survivability testing. In *2018 AIAA/ASCE/AHS/ASC Structures, Structural Dynamics, and Materials Conference*, 2018. DOI: [10.2514/6.2018-0491](https://doi.org/10.2514/6.2018-0491), <https://arc.aiaa.org/doi/abs/10.2514/6.2018-0491>.
- [39] Claudio V. Di Leo, Benjamin León, Jake Wachlin, Martin Kurien, Arjun Krishnan, Ashwin Krishnan, Julian J. Rimoli, and Mark Costello. Design of a crashworthy cable-driven four-bar link robotic landing gear system. *Journal of Aircraft*, 57:224–244, 2020. ISSN: 15333868. DOI: [10.2514/1.C035386](https://doi.org/10.2514/1.C035386).
- [40] Benjamin León, Julian J Rimoli, and Claudio V Di Leo. Ground and Flight Tests of a Cable-Driven Four-Bar Linkage Robotic Landing Gear for Rotorcraft. In *Vertical Flight Society 75th Annual Forum and Technology Display*, 2019.
- [41] Benjamin L. León, Julian J. Rimoli, and Claudio V. Di Leo. Rotorcraft Dynamic Platform Landings Using Robotic Landing Gear. *Journal of Dynamic Systems, Measurement and Control, Transactions of the ASME*, 143, 11 2021. ISSN: 15289028. DOI: [10.1115/1.4051751](https://doi.org/10.1115/1.4051751).
- [42] Sebastian Scherer, Lyle Chamberlain, and Sanjiv Singh. Autonomous landing at unprepared sites by a full-scale helicopter. *Robotics and Autonomous Systems*, 60(12):1545–1562, 2012. ISSN: 0921-8890. DOI: <https://doi.org/10.1016/j.robot.2012.09.004>.
- [43] Mariella Dreissig, Dominik Scheuble, Florian Piewak, and Joschka Boedecker. Survey on LiDAR Perception in Adverse Weather Conditions. In *2023 IEEE Intelligent Vehicles Symposium (IV)*, pages 1–8, 2023. DOI: [10.1109/IV55152.2023.10186539](https://doi.org/10.1109/IV55152.2023.10186539).
- [44] Matt Garratt, Hemanshu Pota, Andrew Lambert, Sebastien Eckersley-Maslin, and Clement Farabet. Visual Tracking and LIDAR Relative Positioning for Automated Launch and Recovery of an Unmanned Rotorcraft from Ships at Sea. *Naval Engineers Journal*, 121:99–110, 6 2009. ISSN: 00281425. DOI: [10.1111/j.1559-3584.2009.00194.x](https://doi.org/10.1111/j.1559-3584.2009.00194.x).

- [45] Sankalp Arora, Sezal Jain, Sebastian Scherer, Stephen Nuske, Lyle Chamberlain, and Sanjiv Singh. Infrastructure-free shipdeck tracking for autonomous landing. In *2013 IEEE International Conference on Robotics and Automation*, pages 323–330, 2013. DOI: [10.1109/ICRA.2013.6630595](https://doi.org/10.1109/ICRA.2013.6630595).
- [46] Shadi Abujoub, Johanna McPhee, and Rishad A. Irani. Methodologies for landing autonomous aerial vehicles on maritime vessels. *Aerospace Science and Technology*, 106, 11 2020. ISSN: 12709638. DOI: [10.1016/j.ast.2020.106169](https://doi.org/10.1016/j.ast.2020.106169).
- [47] Tao Zeng, Hua Wang, Xiucong Sun, Hui Li, Zhen Lu, Feifei Tong, Hao Cheng, Canlun Zheng, and Mengying Zhang. Dual-channel LIDAR Searching, Positioning, Tracking and Landing System for Rotorcraft from Ships at Sea. *Journal of Navigation*, 75:901–927, 7 2022. ISSN: 14697785. DOI: [10.1017/S0373463322000340](https://doi.org/10.1017/S0373463322000340).
- [48] Cezary Kownacki, Leszek Ambroziak, Maciej Ciężkowski, Adam Wolniakowski, Sławomir Romaniuk, Arkadiusz Bożko, and Daniel Ołdziej. Precision Landing Tests of Tethered Multicopter and VTOL UAV on Moving Landing Pad on a Lake. *Sensors*, 23, 2 2023. ISSN: 14248220. DOI: [10.3390/s23042016](https://doi.org/10.3390/s23042016).
- [49] Kewei Xia, Minho Shin, Wonmo Chung, Myunggun Kim, Sangheon Lee, and Hungsun Son. Landing a Quadrotor UAV on a Moving Platform with Sway Motion using Robust Control. *Control Engineering Practice*, 128, 11 2022. ISSN: 09670661. DOI: [10.1016/j.conengprac.2022.105288](https://doi.org/10.1016/j.conengprac.2022.105288).
- [50] Jordan Ross. *The Autonomous Landing of Rotary-Wing UAVs on underway Ships in a Sea State*. PhD thesis, Dalhousie University, 2020.
- [51] Leszek Ambroziak, Maciej Ciężkowski, Adam Wolniakowski, Sławomir Romaniuk, Arkadiusz Bożko, Daniel Ołdziej, and Cezary Kownacki. Experimental Tests of Hybrid VTOL Unmanned Aerial Vehicle designed for Surveillance Missions and Operations in Maritime Conditions from Ship-based Helipads. *Journal of Field Robotics*, 39:203–217, 5 2022. ISSN: 15564967. DOI: [10.1002/rob.22046](https://doi.org/10.1002/rob.22046).
- [52] Linnea Persson and Bo Wahlberg. Model predictive control for autonomous ship landing in a search and rescue scenario. In *AIAA Scitech 2019 Forum*. American Institute of Aeronautics and Astronautics Inc, AIAA, 2019. ISBN: 9781624105784. DOI: [10.2514/6.2019-1169](https://doi.org/10.2514/6.2019-1169).
- [53] Linnea Persson. *Model Predictive Control for Cooperative Rendezvous of Autonomous Unmanned Vehicles*. PhD thesis, KTH Royal Institute of Technology, 2021.
- [54] So-Ryeok Oh, K. Pathak, S.K. Agrawal, H.R. Pota, and M. Garrett. Autonomous Helicopter Landing on a Moving Platform Using a Tether. In *Proceedings of the 2005 IEEE International Conference on Robotics and Automation*, pages 3960–3965, 2005. DOI: [10.1109/ROBOT.2005.1570726](https://doi.org/10.1109/ROBOT.2005.1570726).
- [55] So-Ryeok Oh, K. Pathak, S.K. Agrawal, H.R. Pota, and M. Garratt. Approaches for a Tether-guided Landing of an Autonomous Helicopter. *IEEE Transactions on Robotics*, 22(3):536–544, 2006. DOI: [10.1109/TRO.2006.870657](https://doi.org/10.1109/TRO.2006.870657).
- [56] Bilal Ahmed and Hemanshu R. Pota. Backstepping-based landing control of a RUAV using tether incorporating flapping correction dynamics. In *2008 American Control Conference*, pages 2728–2733, 2008. DOI: [10.1109/ACC.2008.4586905](https://doi.org/10.1109/ACC.2008.4586905).
- [57] L.A. Sandino, D. Santamaria, M. Bejar, A. Viguria, K. Kondak, and A. Ollero. Tether-guided landing of unmanned helicopters without GPS sensors. In *2014 IEEE International Conference on Robotics and Automation (ICRA)*, pages 3096–3101, 2014. DOI: [10.1109/ICRA.2014.6907304](https://doi.org/10.1109/ICRA.2014.6907304).
- [58] Luis Alberto Sandino. *Modeling and Control Techniques of Autonomous helicopters for Landing on Moving Platforms*. PhD thesis, Universidad de Sevilla, 2 2016.
- [59] Francisco Alarcón, Manuel García, Ivan Maza, Antidio Viguria, and Aníbal Ollero. A precise and GNSS-free Landing System on Moving Platforms for Rotary-wing UAVs. *Sensors (Switzerland)*, 19, 2 2019. ISSN: 14248220. DOI: [10.3390/s19040886](https://doi.org/10.3390/s19040886).

- [60] B. I. Schuchardt, T. Dautermann, A. Donkels, S. Krause, N. Peinecke, and G. Schwoch. Maritime Operation of an Unmanned Rotorcraft with Tethered Ship Deck Landing System. *CEAS Aeronautical Journal*, 12:3–11, 1 2021. ISSN: 18695590. DOI: [10.1007/s13272-020-00472-9](https://doi.org/10.1007/s13272-020-00472-9).
- [61] Bianca Isabella Schuchardt, Thomas Dautermann, Alexander Donkels, Teemu Joonas Lieb, Fabian Morscheck, Michael Rudolph, and Gunnar Schwoch. Mission Management and Landing Assistance for an Unmanned Rotorcraft for Maritime Operations. In *2022 IEEE/AIAA 41st Digital Avionics Systems Conference (DASC)*, pages 1–9, 2022. DOI: [10.1109/DASC55683.2022.9925748](https://doi.org/10.1109/DASC55683.2022.9925748).
- [62] Chongfeng Liu, Zixing Jiang, Ruoyu Xu, Xiaoqiang Ji, Lianxin Zhang, and Huihuan Qian. Design and Optimization of a Magnetic Catcher for UAV Landing on Disturbed Aquatic Surface Platforms. In *2022 International Conference on Robotics and Automation (ICRA)*, pages 1162–1168, 2022. DOI: [10.1109/ICRA46639.2022.9812270](https://doi.org/10.1109/ICRA46639.2022.9812270).
- [63] Ruoyu Xu, Chongfeng Liu, Zhongzhong Cao, Yuquan Wang, and Huihuan Qian. A Manipulator-Assisted Multiple UAV Landing System for USV Subject to Disturbance. 12 2022.
- [64] Moritz Maier and Konstantin Kondak. Robot assisted landing of VTOL UAVs on ships: A simulation case study of the touch-down phase. In *2017 IEEE Conference on Control Technology and Applications (CCTA)*, pages 2094–2101, 2017. DOI: [10.1109/CCTA.2017.8062762](https://doi.org/10.1109/CCTA.2017.8062762).
- [65] Moritz Maier, André Oeschger, and Konstantin Kondak. Robot-Assisted Landing of VTOL UAVs: Design and Comparison of Coupled and Decoupling Linear State-Space Control Approaches. *IEEE Robotics and Automation Letters*, 1:114–121, 1 2016. ISSN: 23773766. DOI: [10.1109/LRA.2015.2502920](https://doi.org/10.1109/LRA.2015.2502920).
- [66] Ruoyu Xu, Xiaoqiang Ji, Jiafan Hou, Hengli Liu, and Huihuan Qian. A Predictive Control Method for Stabilizing a Manipulator-based UAV Landing Platform on Fluctuating Marine Surface. In *2021 IEEE/RSJ International Conference on Intelligent Robots and Systems (IROS)*, pages 8625–8632, 2021. DOI: [10.1109/IROS51168.2021.9636055](https://doi.org/10.1109/IROS51168.2021.9636055).
- [67] Botao Hu, Lu Lu, and Sandipan Mishra. Fast, safe and precise landing of a quadrotor on an oscillating platform. In *2015 American Control Conference (ACC)*, pages 3836–3841, 2015. DOI: [10.1109/ACC.2015.7171928](https://doi.org/10.1109/ACC.2015.7171928).
- [68] Botao Hu, Lu Lu, and Sandipan Mishra. A Control Architecture for Fast and Precise Autonomous Landing of a VTOL UAV onto an oscillating platform. In *AHS 71st Annual Forum*, 2015.
- [69] Bruno Herissé, Tarek Hamel, Robert Mahony, and François Xavier Russotto. Landing a VTOL unmanned aerial vehicle on a moving platform using optical flow. *IEEE Transactions on Robotics*, 28:77–89, 2 2012. ISSN: 15523098. DOI: [10.1109/TRO.2011.2163435](https://doi.org/10.1109/TRO.2011.2163435).
- [70] Botao Hu and Sandipan Mishra. Time-Optimal Trajectory Generation for Landing a Quadrotor Onto a Moving Platform. *IEEE/ASME Transactions on Mechatronics*, 24(2):585–596, 2019. DOI: [10.1109/TMECH.2019.2896075](https://doi.org/10.1109/TMECH.2019.2896075).
- [71] Bochan Lee, Vishnu Saj, Dileep Kalathil, and Moble Benedict. Intelligent Vision-based Autonomous Ship Landing of VTOL UAVs. *Journal of the American Helicopter Society*, 68, 4 2023. ISSN: 00028711. DOI: [10.4050/JAHS.68.022010](https://doi.org/10.4050/JAHS.68.022010).
- [72] Bochan Lee, Vishnu Saj, Dileep Kalathil, and Moble Benedict. A Deep Reinforcement Learning Control Strategy for Vision-based Ship Landing of Vertical Flight Aircraft. In *AIAA AVIATION Forum 2021*. American Institute of Aeronautics and Astronautics Inc, AIAA, 2021. ISBN: 9781624106101. DOI: [10.2514/6.2021-3218](https://doi.org/10.2514/6.2021-3218).
- [73] Bochan Lee, Vishnu Saj, and Moble Benedict. Machine Learning Vision and Nonlinear Control Approach for Autonomous Ship Landing of Vertical Flight Aircraft. In *77th Annual National Forum of the Vertical Flight Society*, 2021.

- [74] Tri D. Ngo and Cornel Sultan. Model predictive control for helicopter shipboard operations in the ship airwakes. *Journal of Guidance, Control, and Dynamics*, 39:574–589, 2016. ISSN: 15333884. DOI: [10.2514/1.G001243](https://doi.org/10.2514/1.G001243).
- [75] William B. Greer and Cornel Sultan. Shrinking horizon model predictive control method for helicopter-ship touchdown. *Journal of Guidance, Control, and Dynamics*, 43:884–900, 2020. ISSN: 15333884. DOI: [10.2514/1.G004374](https://doi.org/10.2514/1.G004374).
- [76] Tri D. Ngo and Cornel Sultan. Variable Horizon Model Predictive Control for Helicopter Landing on Moving Decks. *Journal of Guidance, Control, and Dynamics*, 45:774–780, 2022. ISSN: 15333884. DOI: [10.2514/1.G005789](https://doi.org/10.2514/1.G005789).
- [77] Parakh M. Gupta, Eric Pairet, Tiago Nascimento, and Martin Saska. Landing a UAV in Harsh Winds and Turbulent Open Waters. *IEEE Robotics and Automation Letters*, 2 2022. ISSN: 23773766. DOI: [10.1109/LRA.2022.3231831](https://doi.org/10.1109/LRA.2022.3231831).
- [78] Jesse S. Wynn and Timothy W. McLain. Visual Servoing with Feed-Forward for Precision Shipboard Landing of an Autonomous Multirotor. In *2019 American Control Conference (ACC)*, pages 3928–3935, 2019. DOI: [10.23919/ACC.2019.8814694](https://doi.org/10.23919/ACC.2019.8814694).
- [79] Gangik Cho, Joonwon Choi, Geunsik Bae, and Hyondong Oh. Autonomous Ship Deck Landing of a Quadrotor UAV using Feed-forward Image-based Visual Servoing. *Aerospace Science and Technology*, 130, 11 2022. ISSN: 12709638. DOI: [10.1016/j.ast.2022.107869](https://doi.org/10.1016/j.ast.2022.107869).
- [80] Christopher M. Hendrick, Emma R. Jaques, Joseph Francis Horn, Jack W. Langelaan, and Anish Sydney. Evaluation of Autonomous Ship Landing Systems at the Maneuvering and Seakeeping Basin. In *Vertical Flight Society 79th Annual Forum and Technology Display*, 2023.
- [81] Joseph F Horn and J W Langelaan. Experimental Analysis of Advanced Control and Estimation Systems for Autonomous Ship Landing Distribution Statement. Technical report, Office of Naval Research (ONR), 2023.
- [82] Anubhav Datta Abhishek Kumar Shastry and Inderjit Chopra. Vision-based Autonomous UAS Landing on a Stochastically Moving Platform. In *Vertical Flight Society's 77th Annual Forum And Technology Display*, 2021.
- [83] Victoria Britcher, Abhishek Shastry, and Inderjit Chopra. Exploration of Feature-Based Algorithm for Autonomous Ship-Deck Landing under Visually Degraded Conditions. In *Vertical Flight Society's 79th Annual Forum and Technology Display*, 2023.
- [84] Jose Luis Sanchez-Lopez, Jesus Pestana, Srikanth Saripalli, and Pascual Campoy. An Approach toward Visual Autonomous Ship Board Landing of a VTOL UAV. *Journal of Intelligent and Robotic Systems: Theory and Applications*, 74:113–127, 4 2014. ISSN: 09210296. DOI: [10.1007/s10846-013-9926-3](https://doi.org/10.1007/s10846-013-9926-3).
- [85] Alexander D. Jordan, Matthew Rydalch, Tim McLain, and Michael Williamson. *Precision Maritime Localization and Landing with Real-time Kinematic GNSS*. DOI: [10.2514/6.2023-0488](https://doi.org/10.2514/6.2023-0488).
- [86] Adeel Arif, Hesheng Wang, Herman Castaneda, and Yong Wang. Finite-Time Tracking of Moving Platform with Single Camera for Quadrotor Autonomous Landing. *IEEE Transactions on Circuits and Systems I: Regular Papers*, 70:2573–2586, 6 2023. ISSN: 15580806. DOI: [10.1109/TCSI.2023.3256063](https://doi.org/10.1109/TCSI.2023.3256063).
- [87] Yanting Huang, Ming Zhu, Zewei Zheng, and Kin Huat Low. Linear Velocity-Free Visual Servoing Control for Unmanned Helicopter Landing on a Ship With Visibility Constraint. *IEEE Transactions on Systems, Man, and Cybernetics: Systems*, 52:2979–2993, 5 2022. ISSN: 21682232. DOI: [10.1109/TSMC.2021.3062712](https://doi.org/10.1109/TSMC.2021.3062712).
- [88] Biao Wang, Haiwei Lin, Chaoying Tang, and Guili Xu. Autonomous deck landing of a vertical take-off and landing unmanned aerial vehicle based on the tau theory. *Transactions of the Institute of Measurement and Control*, 45(2):233 – 248, 2023. Cited by: 1. DOI: [10.1177/01423312221104424](https://doi.org/10.1177/01423312221104424).

- [89] William K. Holms and Jack W. Lungelaan. Autonomous ship-board landing using monocular vision. In *Annual Forum Proceedings - AHS International*, volume 4, page 3391 – 3405, 2016. DOI: [10.1109/ROBIO54168.2021.9739493](https://doi.org/10.1109/ROBIO54168.2021.9739493).
- [90] Qi Lu, Beibei Ren, and Siva Parameswaran. Shipboard Landing Control Enabled by an Uncertainty and Disturbance Estimator. *Journal of Guidance, Control, and Dynamics*, 41:1502–1520, 7 2018. ISSN: 15333884. DOI: [10.2514/1.G003073](https://doi.org/10.2514/1.G003073).
- [91] Defense Advanced Research Projects Agency. Rotor Buzz UAV description. https://uavrl.com/rotor_buzz_II.html. Accessed: 2023-08-23.
- [92] Jesse Wynn. Visual Servoing for Multirotor Precision Landing in Varying Light Conditions. Master’s thesis, Brigham Young University, 2018.
- [93] André Moura, José Antunes, João J. Martins, André Dias, Alfredo Martins, José M. Almeida, and Eduardo Silva. Autonomous UAV Landing Approach for Marine Operations. pages 1–10. Institute of Electrical and Electronics Engineers (IEEE), 9 2023. DOI: [10.1109/oceanslimerick52467.2023.10244606](https://doi.org/10.1109/oceanslimerick52467.2023.10244606).
- [94] Nguyen Xuan-Mung, Sung Kyung Hong, Ngoc Phi Nguyen, Le Nhu Ngoc Thanh Ha, and Tien-Loc Le. Autonomous Quadcopter Precision Landing onto a Heaving Platform: New Method and Experiment. *IEEE Access*, 8:167192–167202, 2020. DOI: [10.1109/ACCESS.2020.3022881](https://doi.org/10.1109/ACCESS.2020.3022881).
- [95] Nicolò Bastianelli Naticchi, Marco Baglietto, Alessandro Sperindé, Enrico Simetti, and Giuseppe Casalino. Visual Servoed Autonomous Landing on a Surface Vessel. In *OCEANS 2019 - Marseille*, pages 1–8, 2019. DOI: [10.1109/OCEANSE.2019.8867175](https://doi.org/10.1109/OCEANSE.2019.8867175).